FULL ARTICLE

ASSESSMENT OF FAST-SPECTRUM BLANKET LATTICES FOR BREEDING FISSILE FUEL FROM THORIUM AND DEPLETED URANIUM IN AN EXTERNALLY DRIVEN SUB-CRITICAL GAS-COOLED PRESSURE TUBE REACTOR

Blair Patrick Bromley* and Jude Alexander

Canadian Nuclear Laboratories, Chalk River, ON K0J 1J0, Canada.

Article Info
Keywords: thorium, depleted uranium, breeding, sub-critical.
Article History: Received 4 September 2018, Accepted 16 October 2018, Available online 21 November 2018.
DOI: http://dx.doi.org/10.12943/CNR.2018.00010

*Corresponding author: blair.bromley@cnl.ca

To ensure long-term nuclear energy security, it is advantageous to consider the use of externally driven sub-critical systems for producing fissile fuel to supply fleets of thermal-spectrum reactors as an alternative to using fast-spectrum or thermal-spectrum breeder reactors. Computational/analytical neutronics and heat transfer studies have been carried out for gas-cooled fuel bundle lattices with mixtures of fertile thorium and depleted uranium (DU) that could be used in the blanket region of a sub-critical fast reactor driven either by a fusion reactor in a hybrid fusion-fission reactor (HFFR) system, or an accelerator-based spallation neutron source in an accelerator driven system (ADS). The HFFR or ADS concept envisioned is one with a simple cylindrical geometry. The annular-cylindrical blanket is approximately 10 m long, can be made 2–5 m thick (1.0 m ≤ $R_{blanket}$ ≤ 3.0 m to 6.0 m), and is filled with a repeating square lattice of pressure tubes filled with 0.5 m long fuel bundles that are made of (DU,Th)O_2, with various mixtures of Th and DU, and refuelled periodically online. Although using blankets made of pure DUO_2 or ThO_2 are viable options to analyze, mixing DUO_2 with ThO_2 can help alleviate any potential proliferation concerns, since any ^{233}U produced from breeding will be denatured by the presence of ^{238}U in (DU, Th)O_2.

Lattice calculations demonstrate that the total fissile content in the fuel after an extended period of burnup (50 MWd/kg) will be approximately the same, regardless of the mixture of DU and thorium used, and that the content of americium and ^{232}U in the irradiated fuel will be <0.01 wt%/initial heavy metal.

1. Introduction

Within the international community, there are various efforts to investigate using either a fusion reactor [1–9] or an accelerator-driven spallation neutron source [10–13] to drive a sub-critical fast-spectrum reactor to breed excess fissile fuel from depleted uranium (DU) and/or thorium that could be used in conventional thermal-spectrum reactors [14]. Significant stockpiles of depleted uranium (~0.20 wt% $^{235}U/U$) are available from enrichment facilities producing fuel for conventional light-water reactors, whereas thorium is an alternative fertile nuclear fuel that is more than three times as abundant as uranium [15].

A hybrid fusion-fission reactor (HFFR) or an accelerator-driven system (ADS) could be developed to use DU and (or) thorium to produce electrical power, at least to make the system self-sufficient and perhaps to generate excess power to feed to an electrical grid. Such systems could also be adapted to consume and destroy minor actinides (such as isotopes of Am and Cm) found in used nuclear fuel [1, 8–10]. The key advantage of using a fast spectrum for consuming minor actinides (MAs) is that the cross-section for fission in the fast spectrum for several MAs (typically 1 to 2 barns) is higher than that found in the thermal spectrum, and the fission-to-capture ratio is also higher in the fast spectrum, ensuring destruction of MAs rather than conversion into a heavier MA. HFFRs are a potential early application of first-generation fusion reactors. To achieve practical net power generation, a fusion reactor must have a large Q-Value (e.g., $Q = P_{\text{fusion}}/P_{\text{input}} \geq 10$, such as that proposed for the ITER (International Thermonuclear Experimental Reactor) reactor [16]; P_{fusion} is the fusion power; P_{input} is the input heating power), and potentially higher for economical power generation [17]. However, a lower-performance fusion reactor, with $Q \sim 1.0$, may be sufficient to support the operation of a HFFR to produce power and to breed fissile fuel to support a fleet of conventional thermal spectrum fission reactors. Lower-performance fusion reactors may be more feasible and practical to

implement in the near-term. Similarly, an ADS [1, 10–13] may also be used to generate power and breed excess fissile fuel. Both HFFRs and ADS may serve as alternative breeder systems to a fast-breeder reactor and could have the advantage of not requiring an initial reactor loading of high-fissile-content fuel (typically ranging between 10 wt% to 25 wt% fissile fuel/initial heavy metal (IHM) for various types of fast reactor systems [18–20]) to sustain the criticality of the system.

1.1 Incentive for using externally driven sub-critical systems

One simple reason for using an externally driven sub-critical system (either an HFFR or an ADS) to produce power and breed fissile fuel from a blanket containing fertile fuel in the form of DUO_2, ThO_2, or $(DU,Th)O_2$ instead of using a critical reactor is that sub-critical systems do not require the initial fuel to have any fissile fuel. In contrast, fast-spectrum breeder reactors operating on a Pu/U fuel cycle typically require a relatively large fissile content of more than 10 wt% fissile/IHM, just to stay critical [18–20]), and will need a higher fissile content to achieve an acceptable level of fuel burnup. Within a fast-breeder reactor, a portion of the fissile fuel bred in the external blanket will need to be reprocessed and recycled back into the core of the fast breeder reactor to sustain its criticality, leaving less bred fissile material to support the operation of other reactors. Similarly, a thermal-breeder reactor operating on the $^{233}U/Th$ fuel cycle will need an initial fissile enrichment of at least 1.5 wt% $^{233}U/(U+Th)$, and with a relatively small breeding ratio (typically <1.08) [21], there will be little excess fissile material bred to support the operation of other reactors. In contrast, an externally driven sub-critical system does not require the use of any fissile enrichment of the feed fuel going into the blanket; it can be built up over time, and all of the fissile fuel produced can be used subsequently to support a larger fleet of fission reactors, usually thermal-spectrum reactors that require only a low fissile content (usually <5 wt% fissile/IHM) [10, 13, 22].

Another potential advantage of using an HFFR or an ADS is that once the external neutron source is removed by shutting down either the fusion reactor or the accelerator, fissions in the blanket will come to a stop quickly without the need for the insertion of control rods. Thus, the blanket in the ADS or HFFR system can never become super-critical, which gives it a safety advantage relative to thermal and fast breeder reactors.

To a first approximation using a simple one-group neutron balance, the fission power in the blanket of an HFFR is related to the fusion power by the following:

$$\frac{P_{\text{fission}}}{P_{\text{fusion}}} = \frac{E_{\text{fission}}}{E_{\text{fusion}}}\left(\frac{k_{\text{eff}}}{1-k_{\text{eff}}}\right)\frac{1}{\upsilon_{\text{fission}}} \tag{1}$$

P_{fusion} is the power generated by fusion in the fusion reactor component of the HFFR. P_{fission} is the power generated by fission in the blanket containing nuclear fuel (such as $(DU,Th)O_2$). E_{fission} is the recoverable energy released from the fission of fissionable isotope, and E_{fusion} is the energy released from the fusion of two nuclei (such as deuterium (D) and tritium (T)). The parameter k_{eff} is the effective neutron multiplication factor of the blanket. The parameter ν_{fission} is the number neutrons produced per fission in the blanket containing fissionable or fissile material.

In a similar way, the fission power in the blanket of an ADS is related to the accelerator ion beam power by the following:

$$\frac{P_{\text{fission}}}{P_{\text{Beam}}} = \frac{E_{\text{fission}}}{E_{\text{Beam}}}\left(\frac{k_{\text{eff}}}{1-k_{\text{eff}}}\right)\frac{\upsilon_{\text{spallation}}}{\upsilon_{\text{fission}}} \tag{2}$$

P_{beam} is the power of the proton beam ($P_{\text{beam}} = I_{\text{beam}} \times V_{\text{beam}}$, where I_{beam} is the proton beam current and V_{beam} is the proton beam voltage). E_{beam} is the energy of the proton from the accelerator, where $E_{\text{beam}} = q_{\text{proton}} \times V_{\text{beam}}$, where q_{proton} is the charge of a proton. The parameter $\nu_{\text{spallation}}$ is the number spallation neutrons produced proton in the spallation target in the ADS.

Both Equations (1) and (2) are derived from first principles using the steady-state one-group neutron diffusion equation with an external source term, which is either a fusion neutron source or a spallation neutron source. Similar derivations have been found in previous studies [23]. These relationships shown in Equations (1) and (2) are plotted in Figure 1 using $\nu_{\text{fission}} = 2.5$ neutrons/fission and $\nu_{\text{spallation}} =$ 10 and 20 neutrons per proton (n/p), which are a typical values for 1-GeV protons striking a lead-based spallation neutron source target (see Figure 2). Higher values for $\nu_{\text{spallation}}$, up to 40 n/p, may be possible if a uranium-based target is used instead. Sample values for the other

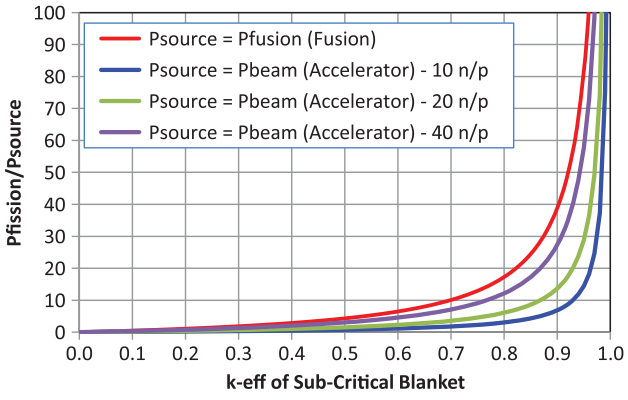

FIGURE 1. Estimated power gain in a sub-critical blanket.

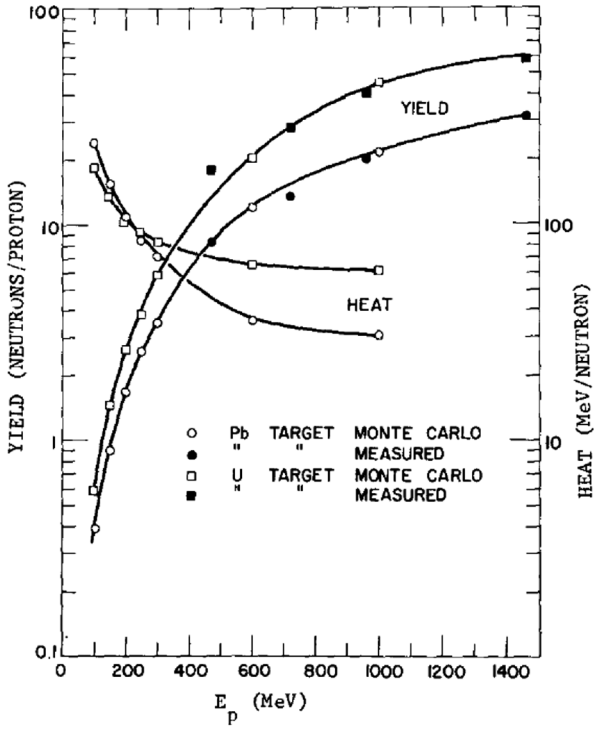

FIGURE 2. Spallation neutron yield from protons on targets (from [13]).

parameters include: $E_{fission} = 190$ MeV (for ^{233}U fission), $E_{fusion} = 17.6$ MeV (for D-T fusion), $E_{beam} = 1000$ MeV (typical for a proton beam in an ADS). The parameter k_{eff} is the effective multiplication of the sub-critical blanket. A significant power gain (≥10) is possible in an HFFR for blankets with $k_{eff} \geq 0.7$, and in an ADS for blankets with $k_{eff} \geq 0.93$ (for $\nu_{spallation} = 10$ n/p), $k_{eff} \geq 0.87$ (for $\nu_{spallation} = 20$ n/p), and $k_{eff} \geq 0.77$ (for $\nu_{spallation} = 40$ n/p).

Equations (1) and (2) can be combined with an assumed input power ($P_{input} = P_{Fusion}/Q$, or $P_{input} = P_{Beam}/\eta_{acc}$), where η_{acc} is the efficiency of the accelerator in converting electrical power into proton beam power, and the net thermodynamic conversion efficiency η_{th} to determine the minimum k_{eff} of the blanket required such that the HFFR or ADS will be self-sustaining in power:

$$P_{net} = \eta_{th} \times (P_{Fission} + P_{Fusion}) - \frac{P_{Fusion}}{Q} \geq 0.0 \quad (3)$$

$$P_{net} = \eta_{th} \times (P_{Fission} + P_{Beam}) - \frac{P_{Beam}}{\eta_{acc}} \geq 0.0 \quad (4)$$

P_{input} is the total input electrical power used to heat and confine the fusion plasma or to operate the accelerator. The net thermodynamic efficiency η_{th} for converting heat to electricity can be adjusted to account for the auxiliary power that would be needed to operate coolant pumps, etc. It is assumed that the energy of the fusion neutrons escaping from the plasma confinement region will be deposited mainly in the blanket fuel and other structural components. It is also assumed that part of the fusion power or the ion beam power dumped on the spallation target can be recovered by thermodynamic conversion in the same way that the heat from the fission power is recovered. Sample results of the minimum k_{eff} required for different conversion efficiencies and Q-values are shown in Figure 3 for an HFFR. For $Q = 1.0$, and $\eta_{th} = 40\%$, $k_{eff} \geq 0.26$ is required for $P_{net}/P_{fusion} \geq 0.0$. A conversion efficiency of $\eta_{th} = 30\%$ is comparable with that achieved currently by conventional pressure-tube heavy-water reactors (PT-HWRs) [24] and some light-water reactors [25], whereas a conversion efficiency of $\eta_{th} = 40\%$ is comparable with that achieved currently by advanced gas-cooled reactors (AGRs) in the U.K. [25]. A conversion efficiency of $\eta_{th} = 50\%$ may be achievable by various advanced reactor technologies operating at high exit coolant temperatures (≥700 °C) and using combined thermodynamic cycles (such as a Brayton/gas turbine and Rankine/steam turbine) or supercritical water cycles [26–28].

Similarly, sample results of the minimum k_{eff} required for different net thermodynamic conversion efficiencies and accelerator efficiencies are shown Figure 4 (for $\nu_{spallation} = 10$ n/p) and Figure 5 (for $\nu_{spallation} = 20$ n/p). The minimum k_{eff} required for an ADS as a function of η_{acc} is also shown in Figure 6 for three different values of $\nu_{spallation}$ (10, 20, 40 n/p) at a nominal net thermodynamic conversion efficiency of 40%. For $\eta_{acc} = 75\%$, $\eta_{th} = 40\%$, and $\nu_{spallation} = 20$ n/p, $k_{eff} \geq 0.606$ is required for $P_{net}/P_{Beam} \geq 0.0$. Because of the limits in spallation neutron production and the efficiency of proton accelerators, there is a significantly higher value of k_{eff} required for the blanket of an ADS than in an HFFR to achieve net power generation.

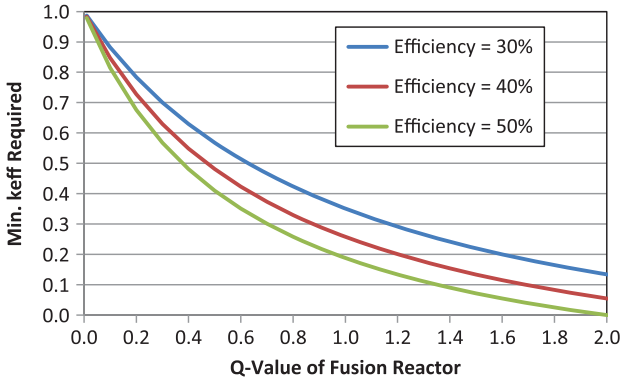

FIGURE 3. Min. k_{eff} required in blanket for net power in HFFR.

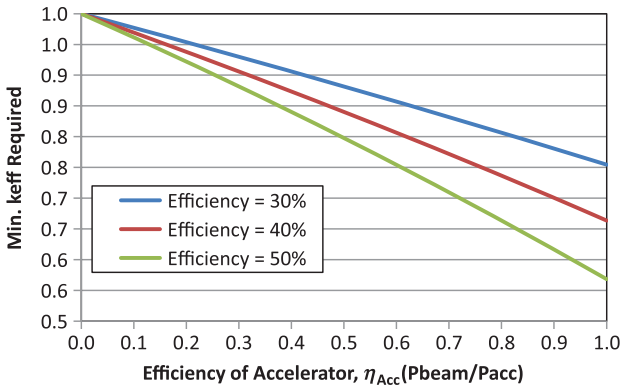

FIGURE 4. Min. k_{eff} required in blanket for net power in ADS with $\nu_{\text{spallation}} = 10$ *n/p*.

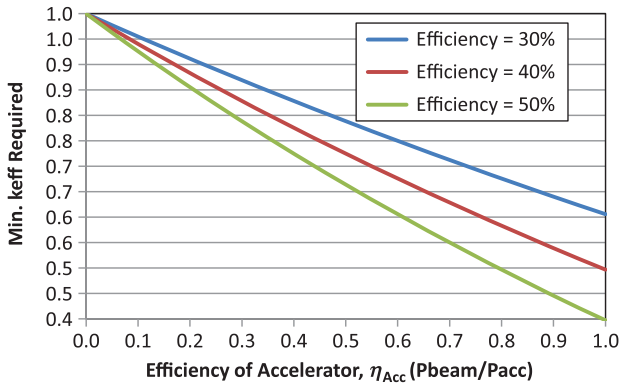

FIGURE 5. Min. k_{eff} required in blanket for net power in ADS with $\nu_{\text{spallation}} = 20$ *n/p*.

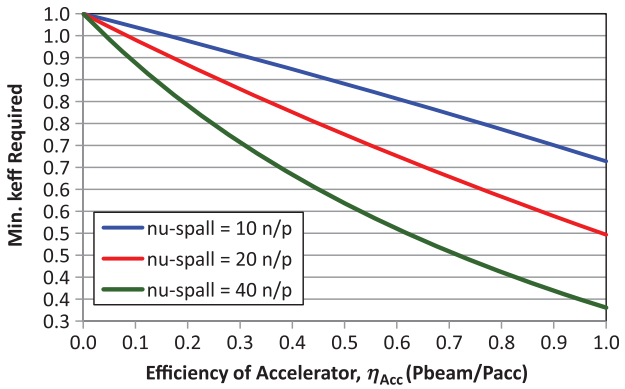

FIGURE 6. Min. k_{eff} required in blanket for net power in ADS with $\eta_{\text{th}} = 40\%$.

1.2 Underlying problem and objective

While both HFFRs and ADS are potential options for breeding fissile fuel for thermal-spectrum reactors, many of the proposed design concepts [2–12] involve the use of fixed blankets that increase in both fissile content and fission power level with time, requiring variable coolant flow rates or reduction of the accelerator or fusion reactor power level, which is neither practical nor cost-effective [29]. In addition, a number of HFFR and ADS concepts [2, 4, 7, 12] involve the use of liquid metal coolants or molten salt blanket fuels/coolants that have added complexity due to corrosion and handling issues. Thus, it is desirable to have a blanket concept that enables online refueling to maintain a constant blanket power, while operating the fusion reactor or accelerator at its maximum level, and it is also desireable to have a blanket system that is practical and feasible in the near-term, making use of existing proven reactor technology. An example of such a technology that could potentially be integrated into an HFFR or ADS system is that of channel-type reactors, such as PT-HWRs and AGRs.

Therefore, the objective of these studies was to carry out preliminary heat transfer/thermal-hydraulic, lattice physics, and blanket neutronic calculations for a variety of lattice concepts that could be used in the blanket of an HFFR or ADS using fuel bundles containing different combinations of $(DU,Th)O_2$ inside pressure tube (PT) fuel channels. These HFFR/ADS blanket concepts would build upon technologies that have been developed for PT-HWRs [24] and gas-cooled reactors, such as the AGR in the United Kingdom [25]. A related objective was to assess the fissile breeding characteristics of a number of HFFR or ADS system concepts with simple homogeneous blanket configurations that are intended to achieve break-even with power production ($P_{\text{net}} \geq 0.0$). The results obtained will provide guidance for developing more detailed calculations of HFFR/ADS sub-critical blankets and for developing modified concepts to achieve enhanced fissile fuel breeding. In previous studies [30], deterministic lattice physics calculations were carried out with WIMS-AECL [31] for a variety of HFFR blanket lattices with fixed initial amounts of ^{233}U in $(^{233}U,Th)O_2$. In this study, the Monte Carlo code Serpent [32, 33] was used instead for lattice physics calculations for fast-spectrum lattices with various combinations of $(DU,Th)O_2$, which could be implemented in either an HFFR or an ADS. The breeding characteristics of a number break-even ($P_{\text{net}} \sim 0.0$) HFFR and ADS systems using these blanket fuels were assessed.

Section 2 provides a description of the HFFR/ADS and the proposed lattice concept for the blanket fuel. Section 3 provides a description of the computational modeling methods and approximations used. Such calculations include the approximate thermal-hydraulic and heat transfer modeling, lattice physics modeling, and blanket neutronics modeling. The thermal-hydraulic calculations provide estimates of the coolant, clad, and fuel temperatures needed for lattice physics calculations. The lattice physics calculations provide estimates of the reactivity of the fuel and the content of key fissile isotopes and a number of elements and isotopes of

interest for radiological or waste management issues (such as americium and ^{232}U). Lattice physics calculations are also used to generate one-group diffusion data for use in blanket neutronics calculations. Blanket neutronics calculations provide estimates of the blanket effective multiplication factor and total blanket power. When used in combination with the burnup-averaged (BU-Ave.) lattice physics data, blanket neutronics analyses can be used to obtain estimates of the refueling rate and production rate of fissile fuel to assess the performance of different blankets in self-sustaining HFFR/ADS systems. Section 4 shows the results of calculations. Sections 5 and 6 provide a summary, conclusions, and a discussion of future options for analyses and improvements.

2. Description of HFFR/ADS Concept

2.1 Fertile blanket concept and driver system

The envisionsed HFFR/ADS concept, as shown in Figure 7, has a relatively simple cylindrical geometry. The external fertile/fissionable blanket has a horizontal orientation, similar to that of fuel channels in a CANDU (CANada Deuterium Uranium) PT-HWR. The central region is approximately 2 m in diameter and 10 m in length and would contain the fusion plasma or the spallation target source. In an HFFR, it is anticipated that a deuterium–tritium (DT) fusion plasma would be confined by a variant of a magnetic mirror fusion reactor (MMFR) [5–7], or some other fusion reactor concept that is compact [34–37] and could fit within the 2-m diameter space. It is also anticipated that the magnetic field coils used to confine the plasma would be placed external to the fertile blanket to protect them from radiation damage. Although such field coils would be large, with a radius of more than 3 m, they are within the range of practical design concepts considered in the past [6, 7]. Some alternative fusion concepts may allow placement of disposable field coils (if they are needed for plasma confinement) between the fertile blanket and the central plasma [38, 39]. Such a fusion reactor would be expected to have a Q-value of at least unity ($Q \sim 1.0$), and would provide 14.1-MeV fast neutrons from the DT fusion reaction, which would drive the surrounding sub-critical blanket made of (DU,Th)O_2 fuel. The surrounding blanket would be 2–4 m thick (1 m $\leq R_{\text{blanket}} \leq$ 3 to 5 m). These values for the blanket thickness were nominal values chosen to minimize the neutron leakage as much as possible, while also being within what is considered practical construction limits. A 3-m outer radius blanket is small enough to fit within the external magnetic field coils of a fusion reactor in an HFFR [6, 7]. A 5-m outer radius blanket is quite large for an ADS system, but comparable in physical size to reactors that have been built in the past, such as the G-2/G-3 prototype reactors in France [40], along with the early Magnox reactors in the U.K. that had core radii ranging between 3 m and 8 m [41].

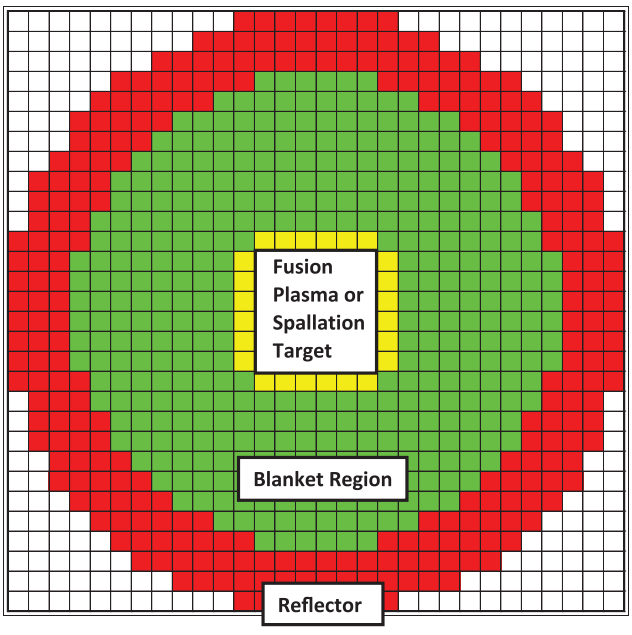

FIGURE 7. Blanket channel layout in sub-critical facility.

The blanket would be surrounded by a reflector/shield region, and the MMFR field coils would be external to the shielding. In an ADS system, no field coils internal or external to the fission blanket would be required. Concepts for lead-based spallation neutron targets for 1-GeV proton beams generated by an external accelerator could be implemented, as discussed in previous studies [10–13]. It is expected that engineering an ADS system would be much more straightforward than an HFFR. While the potential size of the sub-critical blanket, with a 2–4 m thickness and a 10 m length is rather large, it would not be unprecedented. By comparison, the early G-2/G-3 prototype gas-cooled graphite-moderated reactors built in Marcoule, France, in the late 1950s [40] had cores (not including the radial or axial reflectors) that were nearly 8 m in diameter and 8.5 m in length. Specifications for the blanket and lattice concepts are shown in Table 1, and are discussed further below.

2.2 Blanket lattice concept

The blanket in a HFFR/ADS is filled with a repeating lattice (25-cm square pitch) of stainless steel fuel channels filled with 37-element fuel bundles, illustrated in Figure 8. Stainless steel (SS316) is used instead of more traditional zirconium-based alloys because the latter deterioriate in fast-spectrum reactors and will corrode more easily in a high-temperature CO_2 environment. Stainless steel is commonly used for structural components in fast-spectrum reactors [20] and also for the cladding in AGRs, which operate with CO_2 coolant up to temperatures of 650 °C [25].

TABLE 1. HFFR blanket/lattice specifications.

Quantity	Value
Lattice pitch	25 cm
Length of channel	10 m
Length of bundle	50 cm
Length of fuel stack	48 cm
No. of bundles per channel	20
Pressure tube	SS-316
Calandria tube	SS-316
Gap and filler gas	CO_2 at 1 atm
Clad	SS-316
Density of SS-316	8.0 g/cm^3
Coolant	CO_2 (or Ne or Ar) at 11 MPa
Fuel	0 wt% DUO_2, 100 wt% ThO_2 10 wt% DUO_2, 90 wt% ThO_2 20 wt% DUO_2, 80 wt% ThO_2 30 wt% DUO_2, 70 wt% ThO_2 40 wt% DUO_2, 60 wt% ThO_2 50 wt% DUO_2, 50 wt% ThO_2 100 wt% DUO_2, 0 wt% ThO_2
Thorium	100 wt% Th-232
DU	0.1975 wt% U-235/U
Density of fuel	9.7 g/cm^3
No. of fuel pins	37
Fuel pellet radius	0.57 cm
Clad thickness	0.4 mm
Bundle oxide mass	17.584 kg
Bundle fuel HM mass	15.453 to 15.501 kg
Coolant/fuel ratio	1.0
Hydraulic diameter	0.992 cm
PT internal diameter	10.5 cm
PT thickness	0.9 cm
CT Internal diameter	15.8 cm
CT Thickness	0.25 cm
Coolant/fuel area ratio	1.0 to 3.2
Hydraulic diameter	0.99 to 2.55 cm
Nominal channel power	3,000 kW
Nominal coolant mass flow rate	4.97 kg/s
Coolant temperature	250 to 750 °C
blanker inner radius	100 cm
Blanket outer radius	300 to 600 cm
No. of channels for 300-cm blanket	~400
No. of channels for 600-cm blanket)	~17600
Nominal fusion or accelerator beam power	100 MW
Nominal fusion reactor Q-value	1.0
Nominal accelerator efficiency	75%
Nominal efficiency (η_{th})	40%

With a 300-cm outer radius blanket, up to ~400 channels can be accommodated, whereas a 600-cm outer radius blanket will accommodate up to ~1760 channels, each filled with

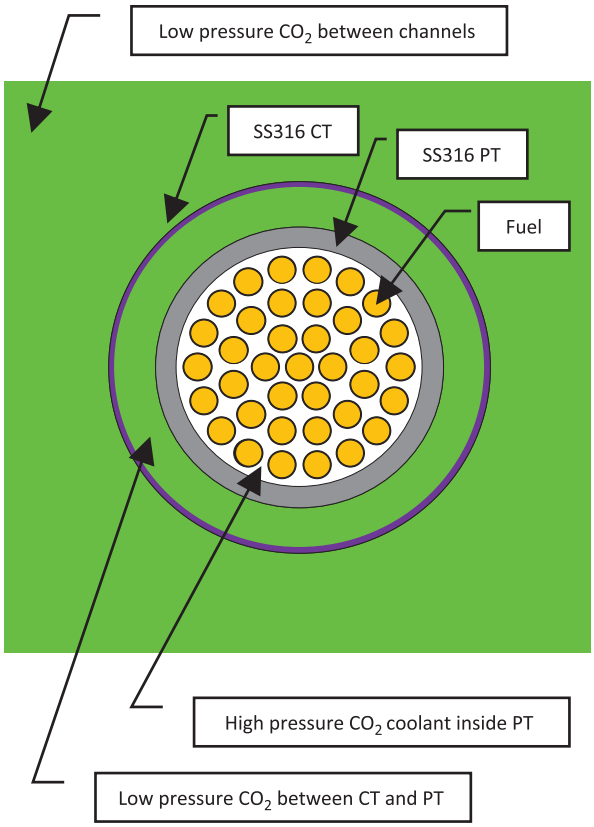

FIGURE 8. 37-CF10 blanket lattice concept (lattice pitch 25 cm).

twenty 50-cm-long blanket bundles. The blanket channel nominal power is assumed to be 3000 kW, which gives an average nominal bundle power of 150 kW (3000 kW/20 bundles). A nominal average bundle power of 150 kW was chosen initially on the basis of achieving a specific power of ~19.5 kW/kg for a different bundle design in a previous study with a heavy metal mass of 7.7 kg [30]. A specific power of 19.5 kW/kg is comparable with that found in other gas-cooled reactors using oxide fuels, such as the EL-4 reactor in France, which operated in France from 1968–1985 [24].

Depending on the neutron flux and power distribution in the blanket, some channels will be at higher or lower power levels. Each fuel bundle is made with (DU,Th)O_2, and the composition varies from 100 wt% ThO_2 to 100 wt% DUO_2, with 7 different compositions to be evaluated. Stainless steel is used for the clad, similar to that which is used in AGRs [25] and the EL-4 reactor [24]. The fuel bundle 37-CF10 has an area ratio of coolant-to-fuel (CF) of approximately 1.0. The fuel bundles are cooled by pressurized CO_2 (or potentially neon or argon) at 11 MPa. This pressure was chosen because it would enhance the cooling capability of the gaseous coolant and would be able to more than double

the coolant density and power removal capacity relative to a conventional AGR, which operates with a CO_2 coolant pressure between 4 and 5 MPa [25]. In addition, conventional PT-HWRs with heavy-water coolant typically operate with a coolant density between 10 and 11 MPa [24]. Thus, PTs designed for PT-HWRs would help guide the design of PTs for the HFFR/ADS system under investigation in this study.

The nominal inlet and outlet temperatures of the coolant are 250 °C and 750 °C, respectively, and could enable high thermal conversion efficiency ($\eta_{th} \geq 40\%$). SS316 stainless steel is commonly used in AGRs, which have CO_2 coolant temperatures up to 650 °C [25], and it is expected that SS316 (or other stainless steel alloys with high Cr-Fe purity and low Ni content) can be successfully used in a 750 °C CO_2 environment with relatively little corrosion or degradation (≤0.4 mm of metal loss) over the lifetime of operation (20–30 years) [42, 43] before refurbishment of the blanket components for the HFFR/ADS.

The lattice/bundle concept shares several technological and engineering similarities with PT-HWRs [24], the prototype gas-cooled heavy water reactor (GCHWR) EL-4 developed in France in the late 1960s [44], and the AGR in the U.K. [25]. With a coolant gas outlet temperature of 645 °C, AGRs achieve a net efficiency ≥41%. Thus, it can be expected that similar efficiencies could be achieved with the HFFR/ADS blanket system proposed. Similar to a PT-HWR lattice, the HFFR/ADS lattices (see Figure 8, Table 1) use a calandria tube (CT) to provide separation and insulation of the PT, but the CT and PT are made of SS316 stainless steel instead of zirconium-based alloys (such as Zircaloy-2 and Zr-2.5Nb). In contrast to a thermal-spectrum PT-HWR, there is no moderator to maintain a fast spectrum for breeding and to suppress fission of any ^{233}U, ^{239}Pu, or ^{241}Pu that is bred in the fuel. Instead, the channels are surrounded by of CO_2 at 1 atm, to act as a filler gas. Specifications for the HFFR blanket and lattices blanket, including the nominal operating conditions are shown in Table 1.

2.3 Advantage of a PT blanket assembly

The key advantage of using a PT/fuel channel approach with solid-fuel bundles for a HFFR/ADS blanket is that it could allow practical online refueling and shuffling to maintain the desired blanket power level and power distribution, while also producing irradiated fuel for subsequent reprocessing and recycling on a daily basis. Other types of HFFR/ADS concepts usually implement a fixed blanket [2–4, 10–12], with blanket fuel being removed and replaced in batch-type operations. However, the tradeoff with this approach is that power levels in the blanket will increase with time as the fissile fuel inventory builds up, and thus, the power level of the fusion reactor or the accelerator beam will need to be adjusted continuously, which may be less cost-effective and practical than by allowing continuous operation with periodic online refueling given the expected large capital cost of an accelerator in an ADS or a fusion reactor in an HFFR [22, 29]. In addition, by using periodic online refueling, the spent fuel from the ADS or HFFR can be removed such that it will have a more uniform composition and the fissile content will be maximized, making it more practical for reprocessing and recycling rather than dealing with a much larger range in fissile fuel content in spent fuel and a larger inventory of fuel to handle and process at one time if batch refueling was employed. Another consideration is that batch-type refueling operations will require periodic shutdowns of the system and disassembly of the blanket system to change out the blanket fuel for subsequent reprocessing. Although it is possible that the blanket batch refueling periods could be synchronized with planned shutdowns for the maintenance of the accelerator or fusion reactor, the ability to refuel the blanket online will provide more flexibility in the ADS or HFFR and will permit constant power operation for both the blanket and the accelerator/fusion driver system. It is recognized that other types of HFFR/ADS concepts could use blankets with fluid-type fuels (such as molten salts, aqueous solutions, or slurries) to enable online refueling in a more compact geometry [45–48], although such systems will have other technological challenges and complexities.

As will be shown later, with the concept proposed, fertile $(DU,Th)O_2$ fuel bundles could be irradiated in the fast spectrum of the HFFR/ADS blanket to exit burnups ranging from ~5.5 MWd/kg to 44 MWd/kg, producing fuel with a fissile content of ranging from ~3.2 wt% fissile/IHM to 7.4 wt% fissile/IHM. This fuel could then be reprocessed for manufacturing new fuel to be used in thermal-spectrum fission reactors. Alternatively, these irradiated fuel bundles (with their stainless steel cladding and other structural components) could potentially be used directly in a conventional PT-HWR without any mechanical or chemical reprocessing. There should be no significant issues for using stainless steel cladding, given that stainless steel cladding is used in AGRs [25] and was also used in the prototype EL-4 GCHWR [44]. To increase the production rate of fissile fuel from the HFFR/ADS, it is preferable to remove the blanket fuel at low burnups (≤5 MWd/kg in a fast spectrum). Although increasing the blanket burnup will increase the fissile content and power generation in the blanket, it will also reduce the overall net fissile production rate. Alternatively, if a heterogeneous blanket was implemented, depleted uranium and thorium could be left in an inner blanket region to achieve higher burnups (≥50 MWd/kg), which would build up a higher fissile content (~8–10 wt%) and enhance neutron multiplication and power generation, while blanket fuel in an outer blanket region could be removed at much lower burnup levels to enhance the breeding rate.

3. Computational Modeling Methods and Approximations

3.1 Thermal-hydraulic and heat transfer modeling

To confirm the heat transfer viability of the blanket lattice concepts, and to obtain estimates of component temperatures for subsequent use in lattice physics calculations, thermal-hydraulic calculations are required. Similar to that described in previous studies [30], approximate estimates of the axial temperature profile of the coolant, clad, and fuel in the gas-cooled fuel bundles were obtained by solving the analytical heat conduction equation combined with the heat transfer coefficient (h) based on local coolant conditions. The heat transfer coefficient was determined using the common Dittus–Boelter correlation, as found in textbook calculations [49, 50]:

$$Nu = 0.023 \times \mathrm{Re}^{0.8} \times \mathrm{Pr}^{0.4}; Nu = \frac{h \times d_H}{k} \tag{5}$$

A simple cosine axial power distribution was assumed, with each fuel pin in the fuel bundle at a given axial position having the same power density as a simplifying approximation. The hydraulic diameter (d_H) of the fuel bundle 37-CF10 is 0.992 cm, as shown in Table 1. The nominal channel power was 3000 kW, and the average bundle power was 150 kW. The mass flow rate ($\mathrm{d}m/\mathrm{d}t$) of the CO_2 coolant was adjusted such that the outlet temperature would be approximately 750 °C. Analytical formulae and correlations [49, 50] were also used to determine the local Reynolds number (Re), friction factor (f), pressure drop ($\mathrm{d}P/\mathrm{d}z$), and pumping power ($d^2W/\mathrm{d}z/\mathrm{d}t$) per unit length of channel:

$$\mathrm{Re} = \frac{\mathrm{v} \times d_H}{\nu} \tag{6}$$

$$f = 0.184 \times \mathrm{Re}^{-0.2} \tag{7}$$

$$\frac{\mathrm{d}P}{\mathrm{d}z} = \frac{f}{d_H} \times \rho \times \frac{\mathrm{v}^2}{2} \tag{8}$$

$$\frac{d^2W}{\mathrm{d}t \times \mathrm{d}z} = \frac{1}{\rho} \times \frac{\mathrm{d}m}{\mathrm{d}t} \times \frac{\mathrm{d}P}{\mathrm{d}z} \tag{9}$$

Equations (8) and (9) can be integrated over the length the channel to obtain the total pressure drop and pumping power. To a first approximation, the pumping power varies as the power of 2.8 of the coolant mass flow rate ($\mathrm{d}W/\mathrm{d}t \propto (\mathrm{d}m/\mathrm{d}t)^{2.8}$). This dependency is due to the fact that the friction factor, f, is given by Equation (7).

3.2 Lattice physics modeling with Serpent 1.1.19

To gain an understanding of the neutron transport and burnup behavior of the 37-CF10 blanket concept with different combinations of $(DU,Th)O_2$, 2-D lattice physics calculations were performed using Serpent Version 1.1.19 [32, 33] with a continuous nuclear data library based on ENDF/B-VII.0. Serpent is a 3-D Monte Carlo neutron transport code with burnup capabilities. An infinite lattice spectrum (zero buckling) was used for the burnup calculations. As an approximation, the impact of the external source neutrons (fusion or spallation) is ignored in the lattice calculations, given that the spectrum of the neutrons in the lattice will be dominated by fission neutrons, and that the fission of the fissile and fissionable isotopes will be dominated by fission neutrons [10]. As an initial approximation, a constant specific power of 19.5 kW/kg was used for burnup calculations, based on previous lattice physics analyses performed with WIMS-AECL [30, 31]. This specific power corresponds to a bundle power of ~302 kW (19.5 kW/kg × 15.5 kg). As discussed earlier, the nominal average bundle power in a 3000-kW fuel channel with 20 bundles is 150 kW, although it could be allowed to reach higher values (such as 300 kW/bundle; 6000 kW per channel) if the coolant flow rate is also adjusted. From the Serpent calculations, various key parameters were obtained for data analysis, including the neutron multiplication factor (k-infinity), the composition of the fuel, and various homogenized one-group diffusion data that could be used subsequently in simplified analytical blanket analyses to be discussed below. Lattice physics calculations will also show the content of elements and isotopes of potential concern for waste management or radiological issues, such as americium and ^{232}U.

3.3 Blanket modeling with a 2-D analytical model

Neutronics modeling of a blanket is needed to obtain estimates of the multiplication factor and power level of a proposed blanket, given a fixed external fast neutron source rate. When used in combination with the lattice physics data, the blanket neutronics analysis can also be used to obtain estimates of the production rate of fissile fuel and the refueling rate required.

A simple, analytical solution of the one-group, 2-D (r,z) steady-state diffusion equation was solved for a homogeneous annular, cylindrical blanket, approximating the concept shown in Figure 7. For the purpose of rapid scoping analyses, the use of a one-group, 2-D analytical model was considered acceptable, although more detailed analyses could potentially be performed with core physics codes, such as Serpent [32, 33], or DONJON [51]. The reflector/shield region was not included in the analytical model. The analytical model was used to determine the neutron flux distribution $\phi(r,z)$, power density distribution $P(r,z)$, and the blanket k_{eff}, and to evaluate the total blanket power for a given fusion or spallation neutron source rate, which in turn are related to the fusion power ($S_{\mathrm{fusion}} = P_{\mathrm{fusion}}/E_{\mathrm{fusion}}$) or the neutron beam power ($S_{\mathrm{spallation}} = P_{\mathrm{beam}}/E_{\mathrm{beam}} \times \nu_{\mathrm{spallation}}$). S_{fusion} is the source rate of fusion neutron production, while $S_{\mathrm{spallation}}$ is the source rate of spallation neutron production. An outer boundary condition of zero neutron flux was imposed at the outer extrapolated radius

and extrapolated length of the blanket. The fusion or spallation neutron source was imposed as an inner blanket radius boundary condition of neutron current, with a cosine axial distribution as an initial approximation. Thus, first-flight collisions of 14-MeV fusion neutrons or the multi-MeV spallation neutrons in the blanket were neglected in this fast diffusion model. Thus, as a simplifying approximation, the fusion or spallation neutrons are modeled as being isotropic and diffusing into the blanket, and having the same neutron energy spectrum as the fission neutrons. Previous studies [10] suggest that the spectra of the external source of fast neutrons does not have a major impact, and thus, a fission spectrum can be considered adequate for scoping studies. The one-group cross-section data for the different (DU,Th)O_2 lattices at each burnup step were obtained from Serpent, which automatically generates such data for a given lattice cell. This analytical approach for blanket modeling was used to provide quick results and bounding estimates to guide future analyses, involving more detailed and complex models and more comprehensive and rigorous methods (such as whole-core 3-D Monte Carlo methods combined with burnup).

The solution of the one-group neutron flux is given by a cosine-Bessel function solution:

$$\phi(r,z) = \cos(\alpha \times z) \times (A_1 I_0(\beta \times r) + A_2 K_0(\beta \times r)) \quad (10)$$

where $\alpha^2 = (\pi/H_{ext})^2$ is the axial buckling defined by the extrapolated length of the blanket, $\beta^2 = B^2 - \alpha^2$ is the radial component of buckling, and $B^2 = (\nu\Sigma_f - \Sigma_a)/D$ is the material buckling. As will be shown later, even with burnups as high as 50 MWd/kg, the (DU,Th)O_2 lattices are sub-critical, with k-infinity ≤0.85. Thus, the radial buckling is negative ($\beta^2 \leq 0$). To achieve a positive total material buckling, and potentially a positive radial buckling, a much higher fissile content in the fuel (≥11 wt% fissile/IHM) would be required, as described in previous studies [30]. The constants A_1 and A_2 were determined from the imposed radial boundary conditions. The neutron flux level is proportional to the fixed fusion neutron source rate for HFFRs, S_{fusion}, or the fixed spallation neutron source rate for ADS, $S_{spallation}$. The local power density and total blanket power are obtained by:

$$P(r,z) = \varphi(r,z) \times E_{fission} \times \Sigma_f \quad (11)$$

$$P_{Blanket} = \int_{z=-H/2}^{z=+H/2} dz \int_{r=Rinner}^{r=Router} 2\pi r dr \times P(r,z) \quad (12)$$

The blanket multiplication factor was obtained using:

$$k_{eff\text{-}Blanket} = \frac{Y}{A + L_r + L_z} \quad (13)$$

Y is the production rate of fast neutrons in the blanket, given by:

$$Y = \int_{z=-H/2}^{z=+H/2} dz \int_{r=Rinner}^{r=Router} 2\pi r dr \times \varphi(r,z) \times \upsilon\Sigma_f \quad (14)$$

A is the absorption rate of neutrons, given by:

$$A = \int_{z=-H/2}^{z=+H/2} dz \int_{r=Rinner}^{r=Router} 2\pi r dr \times \varphi(r,z) \times \Sigma_a \quad (15)$$

L_z is the axial leakage rate of neutrons, given by:

$$L_z = 2 \times \int_{r=Rinner}^{r=Router} 2\pi r dr \times J_z(r, H/2), \quad J_z = -D\frac{\partial \varphi}{\partial z} \quad (16)$$

L_r is the radial leakage rate of neutrons, given by:

$$L_r = 2\pi \times R_{outer} \times \int_{z=-H/2}^{z=+H/2} dz \quad J_r(R_{outer}, z), J_r = -D\frac{\partial \varphi}{\partial r} \quad (17)$$

The key one-group parameters ($\nu\Sigma_f$, Σ_f, Σ_a, D, $\nu_{fission}$, and $E_{fission}$) were obtained from the Serpent calculations at each burnup step, and were subsequently used in the analytical diffusion model for blankets with $R_{outer} = 300$ cm and $R_{outer} = 600$ cm to evaluate the k_{eff}/k_{inf}, and total blanket power as a function of burnup, given a nominal input fusion power or beam power of 100 MW. The value of P_{net} was then evaluated, using assumed values for $Q = 1.0$, $\nu_{spallation} = 20$ n/p, $\eta_{accelerator} = 75\%$, $\eta_{th} = 40\%$, $E_{fusion} = 17.6$ MeV, and $E_{beam} = 1000$ MeV to determine the total output electrical power and the input electrical power required. The actual values of the fission neutron yield ($\nu_{fission}$) and energy released from fission ($E_{fission}$) as a function of burnup may differ from the nominal values ($\nu_{fission} = 2.5$; $E_{fission} \sim 190$ MeV) used in Equations (1) and (2), as described in Section 1.1.

For the HFFR/ADS system proposed, which is modeled as having a single homogeneous composition in the 2-D (r,z) one-group diffusion model, and which uses online refuelling, the physics characteristics of the blanket will actually depend on the BU-Ave. properties of the fuel. However, since the main item of interest is to determine the required exit burnup of the fuel in the blanket, such that the HFFR/ADS system will be self-sustaining ($P_{net}/P_{fusion} \geq 0.0$, or $P_{net}/P_{beam} \geq 0.0$), the BU-Ave. value of P_{net}/P_{fusion} or P_{net}/P_{beam} can be evaluated directly, and the value of burnup where $P_{net} \geq 0.0$ can be identified, rather than evaluating BU-Ave. values of the one-group diffusion data and subsequently evaluating P_{net}/P_{fusion} or P_{net}/P_{beam}.

4. Computational Results

4.1 Thermal-hydraulic and heat transfer calculations

The temperature profiles for 37-CF10 at two different channel powers (3000 kW and 6000 kW) are shown in Figures 9 and 10. The peak fuel centerline, peak and average fuel pellet, and the peak and average clad temperatures are shown in Table 2, along with the estimated pressure drop and pumping power. The peak clad temperature (778 °C, for 37-CF10 in a 6000-kW channel) is well below the melting point of SS-316 (1375 °C). The pressure drop for the 6000-kW channel is more three times that for the 3000-kW channel, whereas the pumping power is more than seven times given that the coolant mass flow rate is nearly doubled for the 6000-kW channel, and as described earlier, the pumping power varies as $dW/dt \propto (dm/dt)^{2.8}$. The low pumping power relative to the channel power (1.1% or less of the total channel power) is due the use of a high coolant pressure (11 MPa) and the large change in the coolant temperature ($\Delta T_{coolant} = 500\ °C$). The impact of pressure-drop loss coefficients due to flow obstructions between bundles and appendages has not been evaluated, but it might be expected to double the pressure drop and pumping power [50]. The average clad temperature (575 °C), and average fuel pellet temperature (634 °C) for the 3000-kW channel were used subsequently in the lattice physics models with Serpent.

Table 2. Thermal-hydraulic conditions.

Property	3000-kW channel	6000-kW channel
Flow rate (kg/s)	4.973	9.947
$T_{cool\text{-}inlet}$ (°C)	250.0	250.0
$T_{cool\text{-}exit}$ (°C)	751.4	751.4
T_{clad} Max. (°C)	773	778
T_{clad} Ave. (°C)	575	585
$T_{fuel\text{-}CL}$ Max. (°C)	903	1125
T_{pellet} Max. (°C)	830	935
T_{pellet} Ave. (°C)	634	713
ΔP (kPa)	129.6	451.4
dW/dt (kW)	9.2	64.3

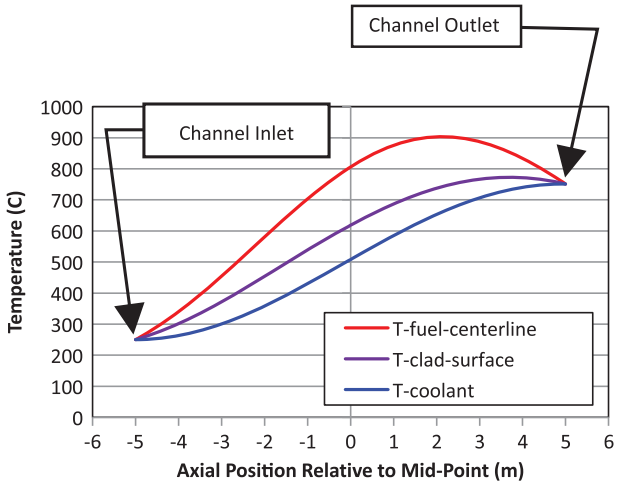

Figure 9. Temperatures in channel 37-CF10 at 3000 kW power.

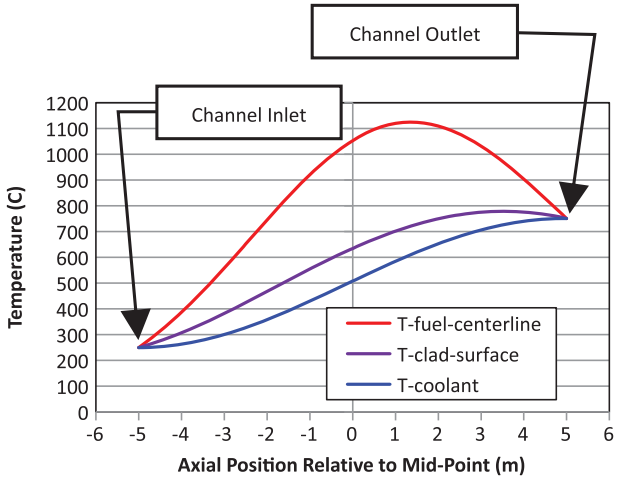

Figure 10. Temperatures in channel 37-CF10 at 6000 kW power.

4.2 Lattice burnup calculations

Results of lattice physics calculations for the various lattices of different combinations of thorium and depleted uranium (100% ThO_2, 10 wt%, 20 wt%, 30 wt%, 40 wt%, 50 wt%, and 100 wt% DUO_2) are shown in Figure 11 and are discussed further below.

4.2.1 Neutron multiplication and fissile content

Plots of k-infinity vs. burnup are shown in Figures 11a and 11b. Plots of total fissile content are shown in Figures 12a and 12b. With little or no initial fissile fuel, the value of k_{inf} starts near zero (≤0.15), increases rapidly in the first 5 MWd/kg of burnup reaching $k_{inf} \geq 0.47$, and then increases more slowly reaching values ≥0.8 after 45 MWd/kg. The case with 100 wt% ThO_2 has values of k_{inf} that exceed all the other cases after a burnup of ~2 MWd/kg, which appears to be high. This result is due to the use of a fixed specific power of 19.5 kW/kg at all burnup levels in the Serpent calculations, which will give an artificially high neutron flux at near-zero burnup, where there is little or no fissile isotopes, allowing a more rapid buildup of ^{233}Th, ^{233}Pa, and ^{233}U. However, by burnup of 5 MWd/kg, when a significant inventory of fissile fuel has been built up (2.8 wt% to 3.8 wt% fissile/IHM), the values of k_{inf} for all cases begin to converge to comparable values

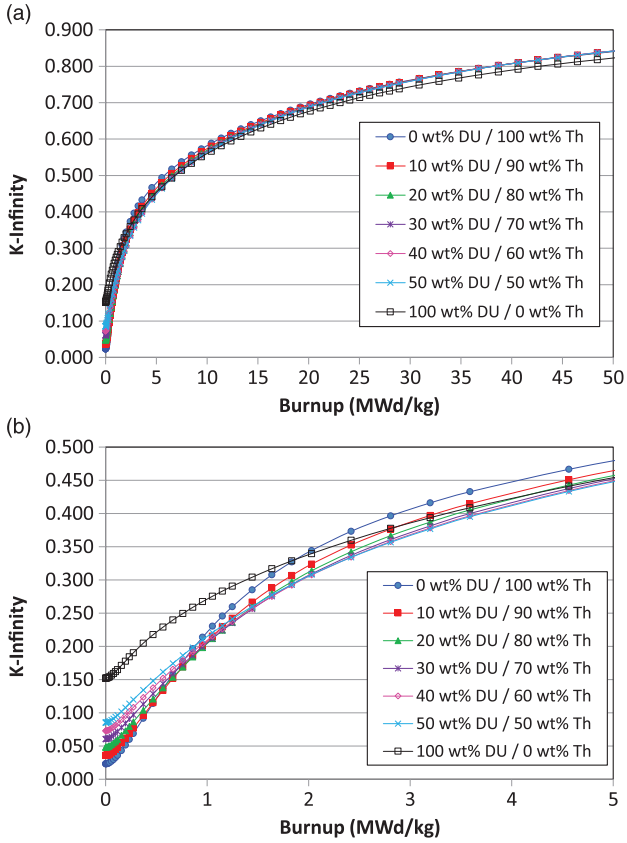

FIGURE 11. k_{inf} vs. burnup. (a) Burnup from 0 to 50 MWd/kg. (b) Burnup from 0 to 5 MWd/kg.

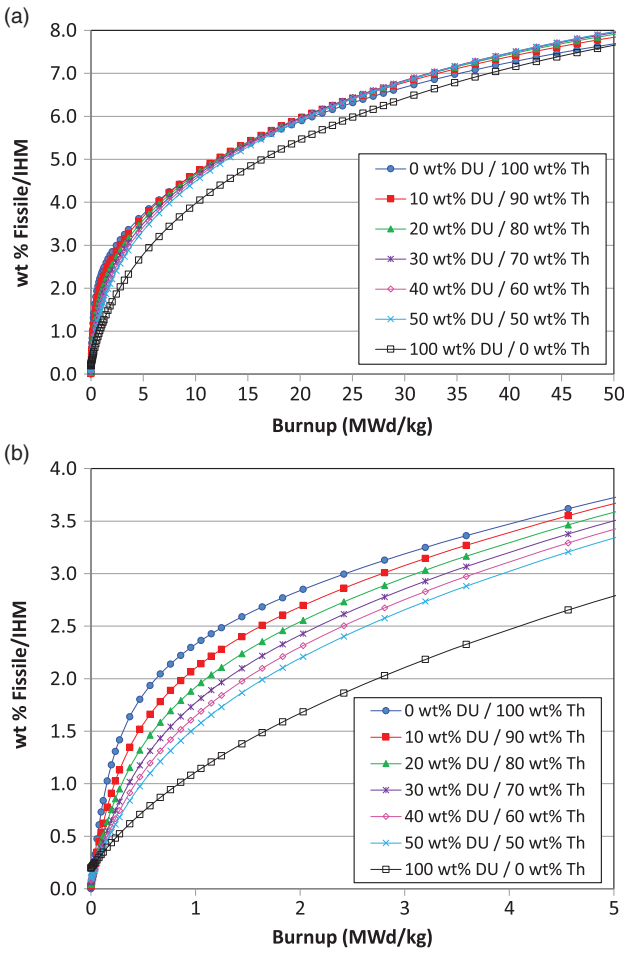

FIGURE 12. Fissile wt% vs. burnup. (a) Burnup from 0 to 50 MWd/kg. (b) Burnup from 0 to 5 MWd/kg.

(0.47–0.49). What is interesting here is that regardless of whether DUO_2 or ThO_2 are used, the values of k_{inf} and total fissile content are quite similar ($k_{inf} = 0.82–0.84$ at 50 MWd/kg), (total fissile content = 7.6–8.0 wt% fissile/IHM) at high burnup (50 MWd/kg), although they are somewhat higher for the lattices with a 50/50 mix of DU and Th. This reactor physics result occurs because of the competing effects of neutron fission and neutron capture in the various fissile isotopes (^{233}U, ^{235}U, ^{239}Pu, and ^{241}Pu) and fertile isotopes (^{232}Th, ^{238}U, ^{234}U, and ^{240}Pu) in a fast neutron energy spectrum where the various neutron fission and neutron capture cross-sections are similar.

Plots of Pu-fissile and U-fissile vs. burnup are shown Figures 13 and 14. The fissile plutonium includes both ^{239}Pu and ^{241}Pu, while the fissile uranium includes ^{233}Pa, ^{233}U, and ^{235}U. The isotope ^{233}Pa is treated as a fissile isotope, since it will decay to ^{233}U. These data clearly show that as the fraction of DU in the $(DU,Th)O_2$ fuel increases, so does the fraction of fissile plutonium in the fuel. For the fuels with thorium, the fissile uranium content increases rapidly in the first 2 MWd/kg of burnup

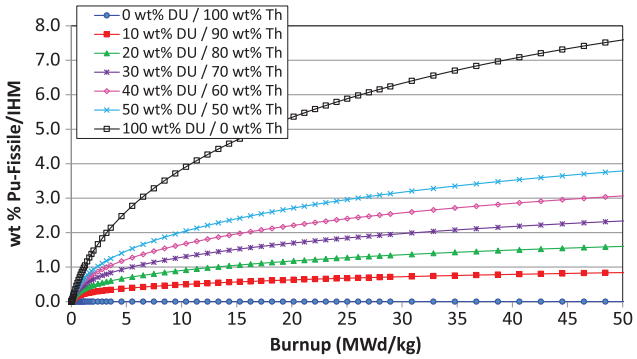

FIGURE 13. Pu-fissile wt% vs. burnup.

(1.3 wt% to 2.8 wt% U-Fissile/IHM), and then grows more slowly as the bred fissile uranium isotopes begin to undergo fission. For the fuel with 50 wt% DUO_2 and 50 wt% ThO_2, the Pu-fissile content reaches ~1.5 wt%, and the U-fissile content reaches ~1.9 wt% at 5 MW/kg.

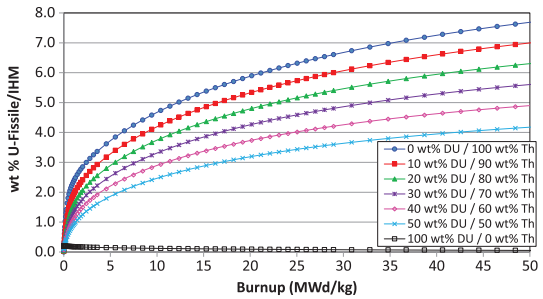

FIGURE 14. U-fissile wt% vs. burnup.

4.2.2 Fissile fraction and minor actinides of interest

Plots of the fraction of Pu-fissile in Pu and U-fissile in U are shown in Figures 15 and 16. As shown in Figure 15, after 5 MWd/kg of burnup, the plutonium is approximately 95.0 to 95.5 wt% fissile, and this value drops down to 84.9 wt% to 87.6 wt% at 50 MWd/kg, being slightly higher for the fuels with ThO_2 mixed in. As shown in Figure 16, for the blanket fuel made of pure ThO_2, the fissile uranium content drops from 100 wt% down to 94 wt% at 5 MWd/kg, and then drops down to approximately 90.5 wt% at 50 MWd/kg. For the fuels with mixtures of DUO_2 and ThO_2, the presence of DU limits the fissile fraction of uranium, ranging between 3.8 wt% and 25.1 wt% U-fissile/U at 5.0 MWd/kg. At 50 MWd/kg, the fissile fraction of uranium ranges from 8.7 wt% and 43 wt% U-fissile/U. If a goal was to limit the fissile uranium fraction to <20 wt%, for potential proliferation concerns, then it would be preferable to use blanket fuels with 30 wt% or more DUO_2 mixed with ThO_2, although with blanket fuel burnups of 5 MWd/kg the use of 20 wt% DUO_2 would be sufficient.

Plots of the total americium (Am-241 + Am-242 + Am-242m + Am-243) and total ^{232}U content in the fuel are shown in Figures 17 and 18, while the fraction of ^{232}U in U is shown in Figure 19. The amount of americium produced may be of

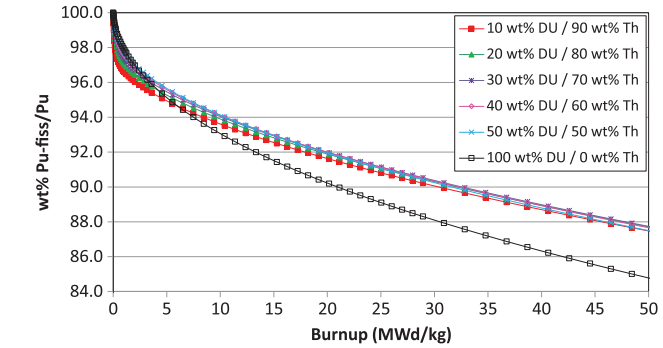

FIGURE 15. wt% Pu-fissile/Pu vs. burnup.

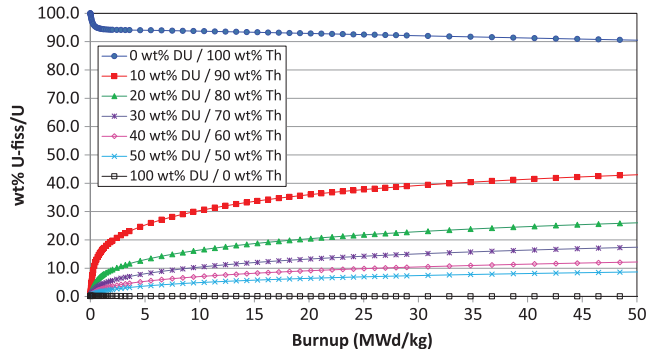

FIGURE 16. wt% U-fissile/U vs. burnup.

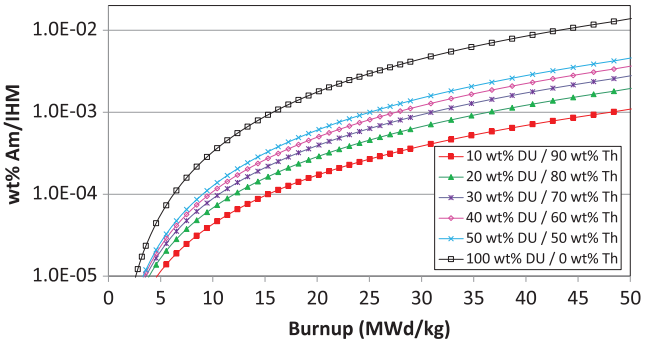

FIGURE 17. wt% Am vs. burnup.

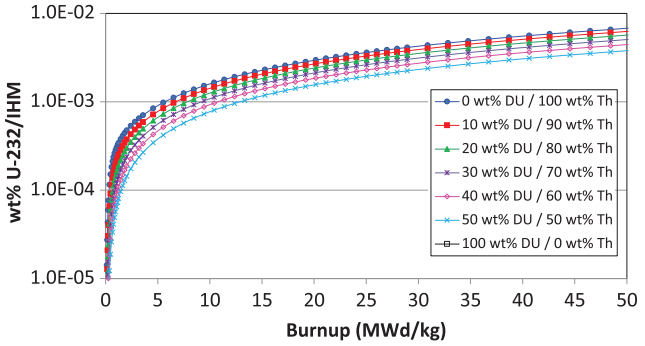

FIGURE 18. wt% ^{232}U vs. burnup.

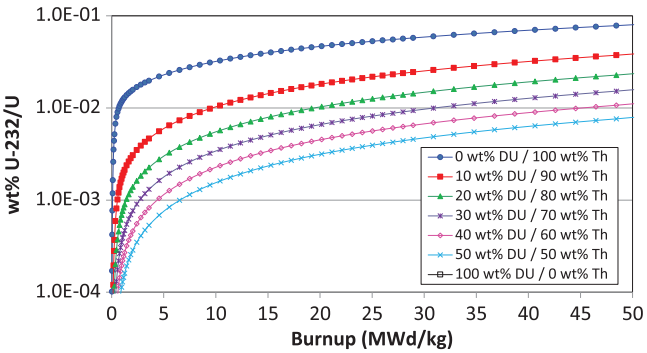

FIGURE 19. wt% $^{232}U/U$ vs. burnup.

concern for long-term waste disposal issues, although it is anticipated that the americium could be recycled and consumed in the same HFFR/ADS facility. The ^{232}U content may be of concern for spent fuel handling and recycling given that one of its radioactive decay chain products, Tl-208, gives off 2.6-MeV gamma rays. As shown in Figure 17, the total americium content is quite low in comparison to the content of the fissile isotopes and varies from 1.4×10^{-5} to 7.3×10^{-5} wt% Am/IHM at a burnup of 5 MWd/kg, while increasing to values ranging from 1.1×10^{-3} to 1.4×10^{-2} wt% Am/IHM at 50 MWd/kg, obviously being highest for the 100 wt% DUO_2 fuel. The amount of americium produced in a pure ThO_2 blanket fuel is negligible. As shown in Figure 18, the ^{232}U content is somewhat higher than the americium content and varies from 3.4×10^{-4} to 7.2×10^{-5} wt% ^{232}U/IHM at a burnup of 5 MWd/kg, while increasing to values ranging 3.8×10^{-3} to 6.8×10^{-3} wt% ^{232}U/IHM at 50 MWd/kg. As shown in Figure 19, the corresponding fraction of ^{232}U in U varies from 6.8×10^{-4} to 2.2×10^{-2} wt% ^{232}U/U at 5 MWd/kg, while increasing to values ranging from 7.9×10^{-3} to 8.0×10^{-2} wt% ^{232}U/U at 50 MWd/kg. The amount of ^{232}U produced in pure DUO_2 fuel is negligible.

4.3 One-group diffusion parameters

Various one-group diffusion parameters, based on the homogenized lattice physics data generated by Serpent, are shown for three fuel types (100 wt% ThO_2, 50 wt% DUO_2/50 wt% ThO_2, and 100 wt% DUO_2) in Figures 20–22. The diffusion coefficient (D) ranges between 5.25 cm at zero burnup for 100 wt% DUO_2 to 5.70 cm for 100 wt% ThO_2 at 50 MWd/kg burnup, as shown in Figure 20. As the DUO_2 content is increased from 0% to 100%, the diffusion coefficient drops by approximately 0.15 cm. As burnup progresses and the content of fissile isotopes increases, while the content of fertile ^{232}Th and ^{238}U decreases, the diffusion coefficient increases by 0.30 to 0.40 cm. The increase with burnup is more significant as the ThO_2 content increases. The migration length ($M = (D/\Sigma_a)^{0.5}$) is quite large in comparison with the migration length found in PT-HWR thermal spectrum lattices (on the order of 15–20 cm [24]), ranging from 86 cm at zero burnup for 100 wt% DUO_2 to 79 cm at 50 MWd/kg burnup for 100% ThO_2, as shown in Figure 21. The large migration length is due to the fast neutron energy spectrum of the blanket, where fast neutrons have a larger migration length in a fast system than neutrons in a thermal-spectrum system. The large migration length is also due in part to the large volume of empty space between the fuel channels that is filled with CO_2 filler gas where there are few neutron interactions. The migration length drops by approximately 6 cm from zero to 50 MWd/kg burnup, and the migration length for ThO_2 is approximately 1.5 cm less than that for DUO_2. The material buckling, $B^2 = (k_{inf}-1)/M^2 = (\nu\Sigma_f-\Sigma_a)/D$, is noticeably negative, ranging from -1.4×10^{-4} cm^{-2} at zero burnup to -2.7×10^{-5} cm^{-2} at 50 MWd/kg, as shown in Figure 22. The values for material buckling for the different

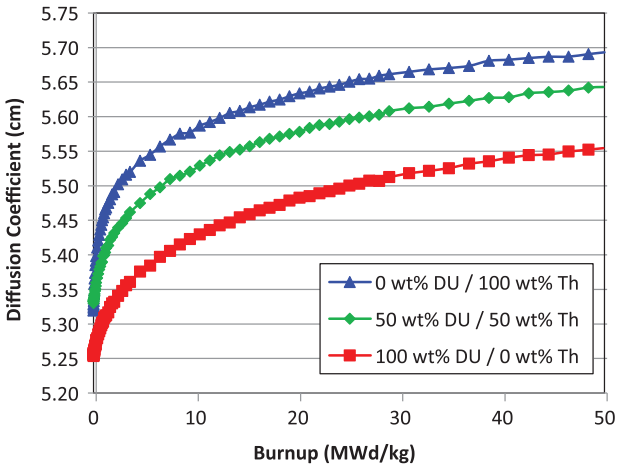

FIGURE 20. Diffusion coefficient for blanket lattices.

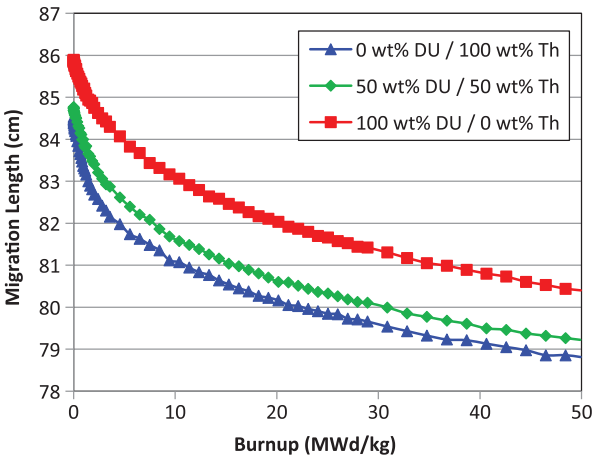

FIGURE 21. Migration length for blanket lattices.

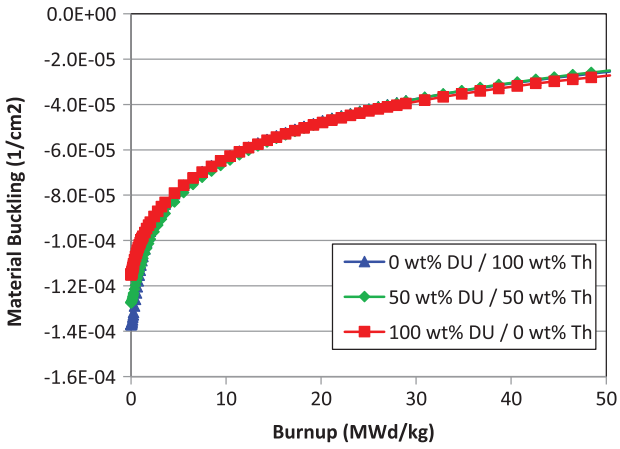

FIGURE 22. Material buckling for blanket lattices.

blanket fuels are quite close and nearly converge by 5 MWd/kg. With comparable values for the diffusion coefficients, migration length, and material buckling, it is expected that the neutron leakage in an associated blanket will be comparable. The one-group homogenized data extracted from the Serpent calculations were used in the subsequent blanket analyses, as discussed in Section 4.4.

4.4 Blanket analyses

Results of the analytical blanket calculations for three blanket fuel types (100 wt% ThO_2, 50 wt% DUO_2/50 wt% ThO_2, and 100 wt% DUO_2) are shown in Figures 23–29. Values of the nonleakage probability (k_{eff}/k_{inf}), based on the homogenized one-group diffusion data for the lattices, and the geometry of the blanket are shown in Figure 23 for a 300-cm-radius blanket, and in Figure 24 for a 600-cm-radius blanket. The nonleakage probability varies from 0.742 for 100 wt% ThO_2 at zero burnup to 0.705 for 100 wt% DUO_2 at 50 MWd/kg burnup. The nonleakage probability decreases by 0.02 to 0.03 in going from zero burnup to 50 MWd/kg burnup. In comparison, in a conventional thermal spectrum reactor [14, 24], the nonleakage probability is on the order of 0.96–0.97 (with a neutron leakage reactivity on the order of 30–35 mk, 1 mk = 100 pcm = 0.001 Δk/k). Thus, the nonleakage probability for this blanket system at 300-cm blanket radius is rather low. This effect occurs because of the large migration length, which is due to the fast neutron energy spectrum, and the large empty space between the fuel channels filled with CO_2. Another reason is that the impact of the radial reflector, which could reduce neutron leakage further, is neglected in the simplified neutronics calculations. If the blanket radius is increased to 600 cm, then the nonleakage probability increases substantially. As shown in Figure 24, the value of k_{eff}/k_{inf} ranges from 0.928 for 100 wt% ThO_2 at zero burnup to 0.907 for 100 wt% DUO_2 at 50 MWd/kg burnup.

Plots of P_{net}/P_{fusion} vs. burnup for the different fuels for a 300-cm-radius blanket, and plots of P_{net}/P_{beam} vs. burnup for the different fuels in a 600-cm-radius blanket are shown in Figures 25 and 26. As discussed earlier, a 300-cm-radius

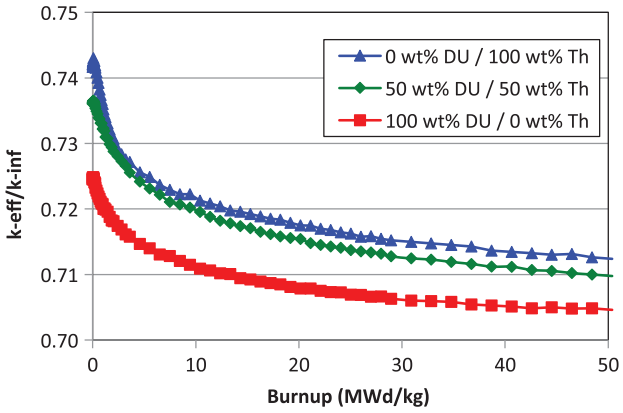

FIGURE 23. k_{eff}/k_{inf} for $R = 300$ cm blanket.

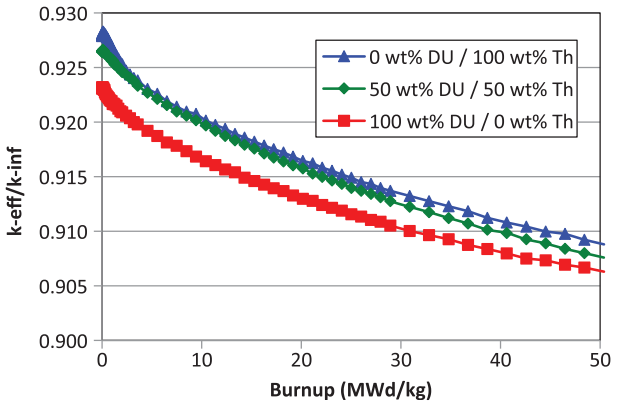

FIGURE 24. k_{eff}/k_{inf} for $R = 600$ cm blanket.

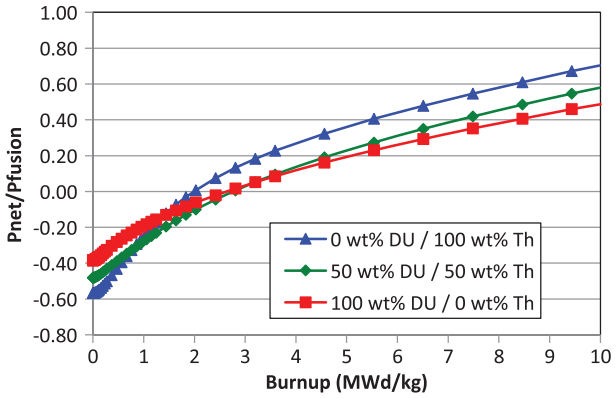

FIGURE 25. P_{net}/P_{fusion} for $R = 300$ cm blanket. Fusion reactor: $Q = 1$.

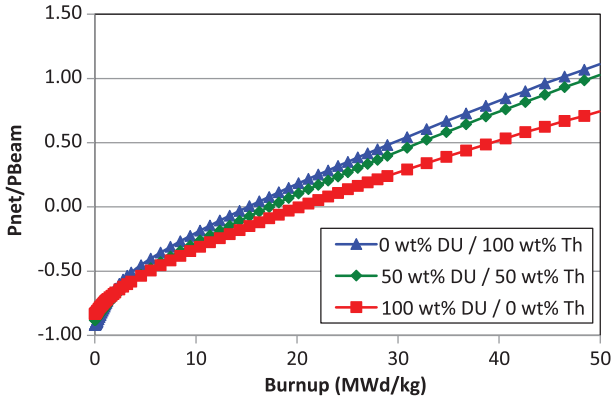

FIGURE 26. P_{net}/P_{beam} for $R = 600$ cm blanket. $\eta_{acc} = 75\%$, $\nu_{spallation} = 20$ neutrons/proton.

blanket was selected for a HFFR due to expected space restrictions imposed by external magnetic field coils. If a single-batch refueling scheme was used for the fusion–neutron-driven blanket, then it is apparent that blanket-average fuel burnup would need to reach at least 2 MWd/kg before net power generation occurs in the blanket with pure ThO_2 and at least 2.8 MWd/kg for the other fuels. For the accelerator-driven system in a 600-cm-radius blanket, positive net power generation would not occur until 15 MWd/kg for ThO_2, 17 MWd/kg for 50 wt% DUO_2/ 50 wt% ThO_2, and 20 MWd/kg for 100 wt% DUO_2.

Given that online refueling of the blanket lattices is to be used, then the fuel will need to be pushed to higher exit burnup to ensure net power generation, since the low reactivity of the fresh blanket fuel needs to be compensated by the higher reactivity of the irradiated blanket fuel. If one refers to Figures 3–6, it is seen that the minimum k_{eff} required for net power generation in a fusion-driven system with $Q = 1.0$ is approximately $k_{eff} \geq 0.258$, whereas the minimum k_{eff} required for net power generation in accelerator-driven system with $\eta_{acc} = 75\%$ and $\nu_{spallation} = 20$ n/p is $k_{eff} \geq 0.606$. If the minimum values for nonleakage probability are assumed for the fuels in the 300-cm-radius ($k_{eff}/k_{inf} \sim 0.712$) and 600-cm-radius ($k_{eff}/k_{inf} \sim 0.909$) blankets, then it is implied that the minimum BU-Ave. k_{inf} for the ThO_2 blanket fuel will need to be BU-Ave. $k_{inf} \geq 0.362$ for the 300-cm HFFR blanket and BU-Ave. $k_{inf} \geq 0.666$ for the 600-cm ADS blanket. From the plot of the BU-ave k_{inf}, as shown in Figure 27, which is based on the data shown earlier in Figure 11, one can interpolate the required discharge burnup. For the HFFR with 100 wt% ThO_2, it appears that a discharge burnup of at least 6.0 MWd/kg is required, whereas for the ADS with 100 wt% ThO_2, a discharge burnup of at least 45 MWd/kg is required. Higher values of burnup will be required for the other fuels. If higher values of nonleakage probability were assumed, then lower discharge burnups would be required.

As mentioned in section 3.3, the BU-Ave. value of P_{net}/P_{fusion} or P_{net}/P_{beam} vs. burnup can be evaluated to get a better estimate of the minimum value of discharge burnup required to ensure net power generation with online refueling. These data were computed based on the data shown in Figures 25 and 26 and plotted as shown in Figures 28 and 29. For the HFFR blanket with online refueling, it appears that net positive power generation occurs when the discharge burnup is greater than 5 MWd/kg for 100 wt% ThO_2 and greater than 6.5 MWd/kg for the 100 wt% DUO_2 fuel. The higher nonleakage probability at low burnup helps. Similarly, for the ADS blanket with online refueling, net positive power generation occurs when the discharge burnup is greater than 33 MWd/kg for ThO_2, 37 MWd/kg for 50 wt% DUO_2 / 50 wt% ThO_2, and 43 MWd/kg for 100 wt% DUO_2.

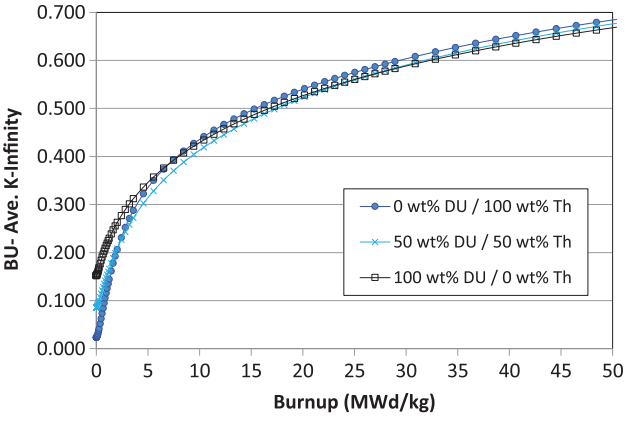

FIGURE 27. BU-Ave. k_{inf}.

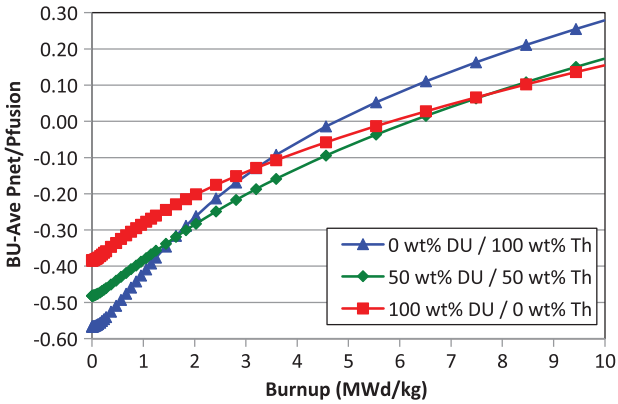

FIGURE 28. BU-Ave. P_{net}/P_{fusion} for $R = 300$ cm blanket (0–10 MWd/kg). Fusion reactor: $Q = 1$, $\eta_{th} = 40\%$.

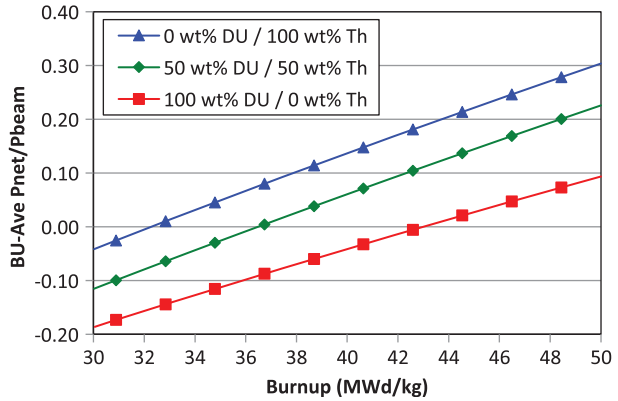

FIGURE 29. BU-Ave. P_{net}/P_{beam} for $R = 600$ cm blanket (30–50 MWd/kg). $\eta_{acc} = 75\%$; $\nu_{spallation} = 20$ neutrons/proton, $\eta_{th} = 40\%$.

4.5 Performance for a break-even HFFR or ADS

Using the data shown in Figures 23–29, along with the data shown in Figure 12, estimates were obtained for the required discharge burnup for several near-break-even HFFR and ADS systems using three types of blanket fuels with online refueling. The results are shown in Table 3 for an HFFR with a 300-cm-radius blanket and in Table 4 for an ADS with a 600-cm-radius blanket. For these calculations, a nominal fusion or beam power of 100 MW was assumed. Included in these tables are estimates of the BU-Ave. total fission power, the total electrical power, input power, net electrical power, the fuel consumption rate, and the net fissile fuel production.

As shown in Table 3, an exit burnup of 5.5 MWd/kg was selected for 100 wt% ThO_2 and 6.5 MWd/kg was selected for the 50 wt% DUO_2/50 wt% ThO_2 and 100 wt% DUO_2 HFFR blankets. With an input fusion power of 100 MWth, the total BU-Ave. fission power ranged from 157 MW to 163 MW, whereas the net electrical power ranged from 1.5 MWe to 5.3 MWe. With the blanket power level and burnup values required, typically between 1.5 and 2 fuel bundles would be replaced each day. The net fissile production per year ranged between 281 kg/year (for 100 wt% DUO_2) to 413 kg/year (for 100 wt% ThO_2). These values are comparable to estimates made in earlier studies [30] using WIMS-AECL for performing the lattice physics calculations.

As shown in Table 4, an exit burnup of 32.8 MWd/kg was selected for 100 wt% ThO_2, 36.7 MWd/kg was selected for the 50 wt% DUO_2/50 wt% ThO_2 and 44.5 MWd/kg was selected for the 100 wt% DUO_2 ADS blankets. With an input beam power of 100 MW, the total BU-Ave. fission power ranged from 236 MW to 239 MW, whereas the net electrical power ranged from 0.4 MWe to 2.1 MWe. With the blanket power level and burnup values required, typically between 0.35 and 0.47 fuel bundles would be replaced each day or one bundle every 2 to 3 days. The net fissile production per year ranged between 144 kg/year (for 100 wt% DUO_2) to 180 kg/year (for 100 wt% ThO_2). The lower production rate of fissile fuel in the ADS relative to the HFFR is due to the

TABLE 3. Estimates of performance of near break-even HFFR with 300-cm radius blanket.

Blanket fuel	0 wt% DU/100 wt% Th	50 wt% DU/50 wt% Th	100 wt% DU/0 wt% Th
Q-value of fusion reactor (P_{fusion}/P_{input})	1.0	1.0	1.0
η_{th}	40%	40%	40%
k_{eff}-min (est.)[a]	0.2578	0.2578	0.2578
H-blanket (m)	10.0	10.0	10.0
R-blanket (cm)	300.0	300.0	300.0
k_{eff}/k_{inf} max[b]	0.742	0.736	0.725
k_{eff}/k_{inf} min[b]	0.712	0.710	0.705
Nominal BU-Ave k_{inf} required, min	0.347	0.350	0.356
Nominal BU-Ave k_{inf} required, max	0.362	0.363	0.366
Nominal BU-Ave k_{inf} selected	0.350	0.351	0.376
Exit BU selected (MWd/kg)	5.538	6.513	6.513
wt% fissile at BU-exit selected	3.846	3.746	3.202
Pfusion (MW) Nominal	100	100	100
Pfission at Exit BU	251.4	237.4	223.1
BU-Ave Pfission at Exit BU	163.1	153.8	156.9
BU-Ave Pfission/Pfusion	1.63	1.54	1.57
Ptotal (MWth)	263.1	253.8	256.9
Pgross (MWe)	105.3	101.5	102.8
Pinput (MWe)	100.0	100.0	100.0
Pnet (MWe)	5.3	1.5	2.8
BU-Ave. P_{net}/P_{fusion}[c]	0.05	0.02	0.03
Mass fuel used (kg/day)	29.457	23.617	24.096
HM Mass of bundle (kg)	15.453	15.477	15.501
Bundles used per day	1.906	1.526	1.554
Bundles used per year	695.763	556.963	567.390
Fissile fuel produced/day (kg/day)	1.133	0.885	0.772
Fissile fuel produced/year (kg/y)	413.545	322.903	281.651

[a] See data in Figure 3.
[b] Non-leakage probability for a 300-cm outer radius blanket. See range of values in Figure 23.
[c] See range of BU-Ave. values in Figure 28.

TABLE 4. Estimates of performance of near break-even ADS with 600-cm radius blanket.

Blanket fuel	0 wt% DU/100 wt%Th	50 wt% DU/50 wt% Th	100 wt% DU/0 wt% Th
$\eta_{Accelerator}$ ($P_{beam}/P_{accelerator}$)	0.75	0.75	0.75
$\nu_{Spallation}$ (neutrons/proton)	20	20	20
η_{th}	40%	40%	40%
k_{eff}-min[a]	0.606	0.606	0.606
H-Blanket (m)	10.0	10.0	10.0
R-Blanket (cm)	600.0	600.0	600.0
k_{eff}/k_{inf} max[b]	0.928	0.926	0.923
k_{eff}/k_{inf} min[b]	0.909	0.908	0.906
Nominal BU-Ave k_{inf} required, min	0.653	0.654	0.656
Nominal BU-Ave k_{inf} required, max	0.666	0.667	0.668
Nominal BU-Ave k_{inf} selected	0.618	0.624	0.650
Exit BU selected (MWd/kg)	32.838	36.738	44.538
wt% fissile at BU-exit selected	6.858	7.280	7.379
Pbeam (MW) nominal	100	100	100
Pfission at Exit BU	384.8	394.2	389.3
BU-Ave Pfission at Exit BU	235.9	234.4	238.6
BU-Ave Pfission/Pbeam	2.36	2.34	2.39
Ptotal (MWth)	335.9	334.4	338.6
Pgross (MWe)	134.4	133.8	135.5
Pinput (MWe)	133.3	133.3	133.3
Pnet (MWe)	1.0	0.4	2.1
Pnet/Pbeam[c]	0.010	0.004	0.020
Mass fuel used (kg/day)	7.184	6.382	5.358
HM Mass of bundle (kg)	15.453	15.477	15.501
Bundles used per day	0.465	0.412	0.346
Bundles used per year	169.7	150.5	126.2
Fissile fuel produced/day (kg/day)	0.493	0.465	0.395
Fissile fuel produced/year (kg/y)	179.824	169.562	144.319

[a] See data in Figure 5.
[b] Non-leakage probability for a 600-cm outer radius blanket. See range of values in Figure 24.
[c] See range of BU-Ave. values in Figure 29.

higher exit burnup required in the ADS to achieve positive net power.

In previous studies of PT-HWRs operating with thorium-based fuels [14], it was found that the net annual consumption of fissile fuel for a 700-MWe PT-HWR operating with (^{233}U,Th)O_2 was approximately 78 kg of fissile uranium per year. Thus, the HFFR with a 300-cm-radius blanket with 100 wt% ThO_2 as feed, producing ~413 kg/year of fissile uranium, could support the operation of at least 5.3 PT-HWRs, whereas the ADS with a 600-cm-radius blanket with 100 wt% ThO_2, producing ~180 kg/year of fissile uranium, could support at least 2.3 PT-HWRs.

To increase the fissile production rate in the HFFR and ADS systems, a number of options are available. The simplest option would be to scale up the fusion power or beam power, and the fission power accordingly. Given that there are on the order of 400 channels in the 300-cm HFFR blanket, with a nominal blanket channel power of 3000 kW (3 MW) one might envision operating an HFFR with a total blanket power of up to 1200 MW (400 × 3 MW), which is far above the 157–163 MW fission power found in the break-even system.

Increasing the size of the blanket further for both HFFR and ADS would be a possibility, although potentially problematic for a HFFR that requires the space for external magnetic field coils. The 600-cm-radius radial blanket for the ADS is already quite large. Alternatively, to increase the neutron multiplication and power level in the blanket without increasing the blanket size or increasing the fusion or beam power, a more heterogeneous blanket concept could be implemented where an inner power-generating blanket could use 10 wt%/IHM fuel, whereas an outer blanket with (DU,Th)O_2 feed fuel would be used for breeding, discharging at lower burnups,

perhaps less than 2 MWd/kg. As shown in previous studies [30], a blanket fuel with 10 wt% ^{233}U/(U+Th) will be in a near-equilibrium state in a fast spectrum (with $k_{inf} \sim 0.99$), and the fissile concentration could be maintained at that level indefinitely.

In addition, the fuel discharged from the HFFR/ADS blanket, which has a fissile content ranging between from 3.2 to 7.4 wt% fissile/IHM, could potentially be used directly in a thermal-spectrum fission reactor such as a PT-HWR without any chemical reprocessing or perhaps any mechanical re-fabrication. Other research groups have proposed similar ideas for creating a tandem system of HFFRs providing fuel for direct use in thermal-spectrum reactors [4, 52]. Extra fissile fuel (^{233}U, ^{239}Pu, and ^{241}Pu) could be built up in the (DU,Th)O_2 fuel to compensate for the added neutron absorption that will occur in the stainless steel clad in a thermal-spectrum reactor such as a PT-HWR.

5. Summary and Conclusions

Computational and analytical studies have been performed to evaluate the characteristics of fertile nuclear fuel in a fast neutron energy spectrum that could be used in the blanket region of either a hybrid fusion–fission reactor or an accelerator-driven system for producing power and breeding fissile fuel, such as ^{233}U, ^{239}Pu, and ^{241}Pu-241. The blanket concept builds upon technology developed for PT-HWRs and gas-cooled reactors, and involves the use of a repeating lattice (25-cm pitch) of 37-element fuel bundles made of (DU,Th)O_2 that are cooled with high-pressure CO_2 gas in PTs. This blanket system would be refueled online, enabling continuous fissile production while operating at constant blanket power. Irradiated fuel discharged from the blanket of the HFFR or ADS would be reprocessed or could potentially be used directly in a thermal-spectrum fission reactor, such as a PT-HWR.

The HFFR concept would only require a low-performance DT-fueled fusion reactor with $Q = 1.0$ for a fast neutron source, while the ADS concept would require an accelerator with an efficiency of $\eta_{acc} = 75\%$, using a 1000-MeV proton beam on a lead-based spallation target producing 20 neutrons/proton. The blanket region, which is filled with 400 to 1760 fuel channels, would have a cylindrical geometry.

Lattice physics calculations were performed using Serpent, while 2-D, one-group diffusion analytical model was used to evaluate the characteristics of the blanket region, driven either by a fusion or accelerator-based spallation fast neutron source.

Several fuel combinations were evaluated, ranging from 100 wt% ThO_2 to 100 wt% DUO_2. Regardless of the fuel combination, the lattice reactivity and total fissile content as a function of burnup were quite similar in a fast spectrum, with k_{inf} ranging from $\sim 0.47 \pm 0.02$ at 5 MWd/kg to $\sim 0.83 \pm 0.02$ at 50 MWd/kg, and the fissile content ranging from $\sim 3.3 \pm 0.5$ wt% fissile/IHM at 5 MWd/kg to $\sim 7.8 \pm 0.2$ wt% fissile/IHM at 50 MWd/kg. The use of a fast neutron spectrum helps to suppress fission the fissile fuel that is bred. The content of americium and ^{232}U in the various lattice concepts is less than 0.01 wt%/IHM.

For the HFFR concept with a 300-cm-radius, 400-channel external blanket with online refuelling to be energy self-sustaining, the blanket fuel would need to be discharged at burnup ranging from 5.5 MWd/kg (for pure ThO_2) to 6.5 MWd/kg (for pure DUO_2). With a 100-MW fusion neutron source, up to 413 kg/year of fission uranium could be produced. For the ADS concept with a 600-cm radius, 1720-channel external blanket to be energy self-sustaining, the blanket fuel would need to be discharged at higher burnups, ranging from 32.8 MWd/kg (for pure ThO_2) to 44.5 MWd/kg (for pure DUO_2). With a 100-MW accelerator proton beam power driving a lead-based spallation neutron source, up to 179 kg/year of fissile uranium could be produced. The amount of fissile uranium produced for the HFFR and ADS systems could support the operation of two to five 700-MWe-class PT-HWRs operating with (^{233}U,Th)O_2 fuel.

If a fusion reactor with $Q = 1.0$ could be developed to fit within the specified blanket geometry, with a 2-m thick and 10-m long blanket made of fuel channels in PTs, then a HFFR operating with ThO_2 blanket fuel as feed fuel would be a highly desirable option for breeding fissile uranium.

6. Future Options

Future studies of fast-spectrum blankets for HFFR and ADS could involve the use of more rigorous neutron transport methods such as Serpent [32, 33] and (or) MCNP [53] for performing 3-D simulations of HFFR/ADS blankets with a source-driven model representative of fusion or spallation neutron sources. Modifications to the blanket concept to increase the reactivity and breeding rate could be evaluated, such as heterogeneous blankets with dedicated power generation and breeding regions. To increase the nonleakage probability of the blanket without increasing the blanket size, the use of smaller-pitch lattices (such as 18-cm square pitch) could be considered, which would reduce the migration length of the lattice. However, such a modification may require shifting to off-line batch refuelling due to the limited space available for the numerous piping and connections in the coolant circuit required for online refueling. Alternatively, a thermal-spectrum blanket lattice could be implemented, using a blanket lattice moderated by heavy water or graphite, which would significantly reduce the

diffusion coefficient and migration length (to values <20 cm for heavy-water lattices). However, the tradeoff with thermal-spectrum lattices is that fission would not be suppressed, and the maximum fissile content that could be achieved in discharged irradiated ThO_2 blanket fuel would be less than 1.4 wt% U-fissile/(U+Th), as observed in previous studies of heterogeneous seed/blanket PT-HWR cores [54, 55, 56]. Finally, studies could be carried out to investigate the characteristics of a tandem HFFR/ADS-PT-HWR system, where thorium-based fuels are recycled directly back-and-forth between a fast-spectrum breeder system (HFFR/ADS) and a fleet of thermal-spectrum power generation reactors (such as PT-HWRs), without chemical reprocessing of the fuel. In such a system, the HFFR/ADS would be used to rejuvenate the fissile content in the fuel, similar to what has been proposed in previous studies [4, 52].

Acknowledgements

The authors thank the following individuals for their help and assistance: G.W.R. Edwards, F.P. Adams, S. Golesorkhi, T. Wilson, S. Pfeiffer, P. Pfeiffer, J. Pencer, S. Livingstone, D.D. Radford, B. Sanderson (Canadian Nuclear Laboratories), and Y. Gohar (Argonne National Laboratory). Funding for this work was provided by the Canadian Nuclear Laboratory's Federal Science and Technology program, which is administered by Atomic Energy of Canada Limited on behalf of the Government of Canada.

References

[1] B.P. Bromley, 2013, "Review of AECL and International Work on Sub-Critical Blankets Driven by Accelerator-Based and Fusion Neutron Sources", Proc. of 34th Annual Conference of the Canadian Nuclear Society, Toronto, ON, Canada, 9–12 June 2013.

[2] C.M. Sommer, W.M. Stacey, and B. Petrovic, 2011, "Fuel Cycle Analysis of the SABR Fusion Fission Hybrid Burner Reactor", ANS Transactions, 104, pp. 699.

[3] A. Talamo and Y. Gohar, 2012, "Neutronics Performance of Pebble Fuel for ^{233}U Production in Fusion Driven Systems", ANS Transactions, 107, pp. 1020.

[4] M. Fratoni, R.W. Moir, K.J. Kramer, J.F. Latkowski, W.R. Meier, and J.J. Powers, 2012, "Fusion-Fission Hybrid for Fissile Fuel Production without Processing", LLNL-TR-522137, Lawrence Livermore National Laboratory, Livermore, CA, USA.

[5] D. Ryutov, A.W. Molvik, and T.C. Simonen, 2010, "Axisymmetric Mirror as a Driver for a Fusion—Fission Hybrid: Physics Issues", Journal of Fusion Energy, 29(6), pp. 548–552. doi: 10.1007/s10894-010-9328-5.

[6] R.W. Moir, (ed.), 1979, "Interim Report on the Tandem Mirror Hybrid Design Study", UCID-18078, Lawrence Livermore Laboratory, Livermore, CA, USA.

[7] R.W. Moir, 1978, "Mirror Hybrid Reactors", UCRL-81611, Lawrence Livermore Laboratory, Livermore, CA, USA.

[8] L.M. Lidsky, 1975, "Fission-Fusion Systems: Hybrid, Symbiotic, and Augean", Nuclear Fusion, 15, pp. 151–173. doi: 10.1088/0029-5515/15/1/016.

[9] H. Bethe, 1979, "The Fusion Hybrid", Physics Today, 32(5), pp. 44–51. doi: 10.1063/1.2995553.

[10] N. Brown, J. Powers, M. Todosow, M. Fratoni, H. Ludewig, E. Sunny, et al., 2016, "Thorium Fuel Cycles with Externally Driven Systems", ANS Nuclear Technology, 194(2), pp. 233–251. doi: 10.13182/NT15-40.

[11] X. Shang, J. Song, Y. Wang, J. Li, G. Yu, and K. Wang, 2017, "Subcritical Multiplication Factor and Burnup Analysis of ADS with RMC", ANS Transactions, 117, pp. 690–693.

[12] H. Takahashi, 1997, "Brookhaven National Laboratory ADS concepts (USA)", IAEA-TECDOC-985, International Atomic Energy Agency (IAEA), Vienna, Austria.

[13] G.A. Bartholomew, J.S. Fraser, and P.M. Garvey, 1978, "Accelerator Breeder Concept", AECL-6363, INFCE/WG.8/CAN/DOC1, International Atomic Energy Agency, Vienna, Austria.

[14] A.V. Colton and B.P. Bromley, 2018, "Simulations of Pressure-Tube-Heavy-Water Reactor Cores Fueled with Thorium-Based Mixed-Oxide Fuels", Nuclear Technology, 203, pp. 146–172, doi: 10.1080/00295450.2018.1444898.

[15] OECD Nuclear Energy Agency and the International Atomic Energy Agency, 2014, "Uranium 2014: Resources, Production and Demand (The Red Book)".

[16] ITER, 2018, "Facts and Figures", Accessed from https://www.iter.org/factsfigures.

[17] "Fusion Energy Gain Factor", 2018, Accessed online from https://en.wikipedia.org/wiki/Fusion_energy_gain_factor.

[18] L. Cinotti, G. Grasso, and P. Agostini, 2017, "Flexibility of the LFR: an ASSET for Novel, Affordable LFR-AS-200-Based SMRs", ANS Transactions, 117, pp. 1464–1467.

[19] M. Martin, M. Aufiero, E. Greenspan, and M. Fratoni, 2017, "Feasibility of Breed-and-Burn Molten Salt Reactor", ANS Transactions, 116, pp. 1174–1365.

[20] IAEA, 2012, "Status of Fast Reactor Research and Technology Development", IAEA-TECDOC-1691, International Atomic Energy Agency, Vienna, Austria.

[21] IAEA, 1979, "Status and Prospects of Thermal Breeders and Their Effect on Fuel Utilization", Technical Report Series No. 195, IAEA, Vienna, Austria.

[22] J.S. Geiger and G.A. Bartholomew, 1981, "A Review of the Prospects for Fusion Breeding of Fissile Material", AECL-7259.

[23] S. Yongqian, D. Dazhao, L. Zhangling, X. Xiaoqin, Z. Yushan, Z. Zhixiang, S. Qingbiao, et al., 1997, "A Conceptual Study of Hybrid System for Nuclear Energy Generation and Transmutation at CIAE", Proceedings of the International Atomic Energy Agency Technical Committee Meeting—Feasibility and Motivation for Hybrid Concepts for Nuclear Energy and Transmutation, IAEA-TC-903.3, Madrid, Spain, 17–19 September 1997, pp. 249–276.

[24] IAEA, 2002, Heavy Water Reactors: Status and Projected Development, IAEA Technical Report Series No. 407, International Atomic Energy Agency, Vienna, Austria.

[25] IAEA, 1976, Directory of Nuclear Reactors, International Atomic Energy Agency, Vienna, Austria, pp. 313–323.

[26] C.F. McDonald, 2014, "Power conversion system considerations for a high efficiency small modular nuclear gas turbine combined cycle power plant concept (NGTCC)", Applied Thermal Engineering, 73(1), pp. 82–103. doi: 10.1016/j.applthermaleng.2014.07.011.

[27] E.A. Harvego and M.G. McKellar, 2011, "Optimization and Comparison of Direct and Indirect Supercritical Carbon Dioxide Power Plant Cycles for Nuclear Applications", INL/CON–11-21227, Idaho National Laboratory, Idaho Falls, ID, USA.

[28] L.K.H. Leung, M. Yetisir, W. Diamond, D. Martin, J. Pencer, B. Hyland, et al., 2011, "A Next Generation Heavy Water Nuclear Reactor With Supercritical Water As Coolant", CW-127000-CONF-002, Proceedings of the International Conference on the Future of Heavy Water Reactors, Ottawa, ON, Canada, 2–5 October 2011.

[29] Y. Gohar, Y. Cao, and A. Kraus, 2018, "Accelerator-Driven Subcritical System for Disposing of the U.S. Spent Nuclear Fuel Inventory", ANL-18/07, Argonne National Laboratory, Lemont, IL, USA.

[30] B.P. Bromley, 2015, "Studies of Pressure-Tube Blanket Lattices with Thorium-Based Fuels for a Hybrid Fusion-Fission Reactor", Fusion Science and Technology, 68(3), pp. 546–560. doi: 10.13182/FST14-851.
[31] Altiparmakov, D.V., 2008, "New Capabilities of the Lattice Code WIMS-AECL", International Conference on the Physics of Reactors, Interlaken, Switzerland, September 2008, American Nuclear Society.
[32] J. Leppanen and M. Dehart, 2009, "HTGR Reactor Physics and Burnup Calculations Using the SERPENT Monte Carlo Code," ANS Transactions, 101, pp. 782.
[33] J. Leppänen, 2012, "PSG2/Serpent—a Continuous-energy Monte Carlo Reactor Physics Burnup Calculation Code", 5 March 2012. Available for download at www.montecarlo.vtt.fi.
[34] S.B. Nickerson, W.T. Shmayda, P.J. Dinner, and P. Gierszewski, 1984, "Review of Compact, Alternate Concepts for Magnetic Confinement Fusion", Ontario Hydro Report F83029, Canadian Fusion Fuels Technology Project (CFFTP), Mississauga, ON, Canada.
[35] P.J. Gierszewski, A.A. Harms, and S.B. Nickerson, 1990, "Alternate Fusion Concepts", CFFTP-G-9009, Canadian Fusion Fuels Technology Project, Mississauga, ON, Canada.
[36] D. Clery, 2014, "Fusion's Restless Pioneers", Science, 345(6195), pp. 370–375. doi: 10.1126/science.345.6195.370. PMID: 25061186.
[37] M. Waldrop, 2014, "The Fusion Upstarts", Nature, 511(7510), pp. 398–400. doi: 10.1038/511398a. PMID: 25056045.
[38] M. Kotschenreuther, S. Mahajan, P. Valanju, B. Covele, S. Pratap, M. Werst, et al., 2010, "Nearer Term Fission-Fusion Hybrids: Recent Results", Proceedings of the 23rd IAEA Fusion Energy Conference, Daejeon, South Korea, 11–16 October 2010, pp. 414–415.
[39] M. Kotschenreuther, P. Valanju, and S. Mahajan, 2012, "Reprocessing Free Nuclear Fuel Production via Fusion Fission Hybrids", Fusion Engineering and Design, 87, pp. 303–317. doi: 10.1016/j.fusengdes.2012.01.004.
[40] IAEA, 1962, "Reactors G-2 and G-3", Directory of Nuclear Reactors, vol. IV, International Atomic Energy Agency, Vienna, Austria, pp. 191–196.
[41] IAEA, 1962, "Dungeness Nuclear Power Station", Directory of Nuclear Reactors, vol. IV, International Atomic Energy Agency, Vienna, Austria, pp. 261–266.
[42] A.N. Charcharos and A.G. Jones, 1984, "Design and development of steam generators for the AGR power stations at Heysham II/Torness", Paper 58, Proceedings oInternational Working Group on Gas-Cooled Reactors, Specialists' meeting on heat exchanging components of gas-cooled reactors (WGGCR-9), Duesseldorf, Germany, 16–19 April 1984, International Atomic Energy Agency (IAEA), Vienna, Austria, pp. 204–217.
[43] K. Yasuyoshi, N. Takeshi, and Y. Yoshio, 2001, "A carbon dioxide partial condensation direct cycle for advanced gas cooled fast and thermal reactors", Proceedings of Global 2001 international conference on: "back-end of the fuel cycle: from research to solutions", INIS-FR-1118, Paris, France, 9–13 September 2001.
[44] IAEA, 1968, Directory of Nuclear Reactors, International Atomic Energy Agency, Vienna, Austria, pp. 259–288.
[45] P. McIntyre, A. Sattarov, P. Tsvetkov, W. Horak, et al., 2011, "Neutronics and Heat Transfer for an ADS Molten Salt Core", ANS Transactions, 105, pp. 17–18.
[46] P. McIntyre, E. Sooby, P. Tripathy, M. Simpson, and S. Phongikaroon, 2011, "Candidate Heavy Salt Systems for Accelerator-Driven Sub-Critical Molten Salt Fission", ANS Transactions, 105, pp. 405–406.
[47] A. Talamo and Y. Gohar, 2012, "^{233}U Production by Fusion Driven Systems Using Slurry Fuel Carrier", ANS Transactions, 106, pp. 695–696.
[48] W. Manheimer, 2004, "The Fusion Hybrid as a Key to Sustainable Development", Journal of Fusion Energy, 23(4), pp. 223–235. doi: 10.1007/s10894-005-5615-y.
[49] M.M. El-Wakil, 1993, Nuclear Heat Transport, 3rd ed, American Nuclear Society, La Grange Park, IL, USA.
[50] N. Todreas and M. Kazimi, 1993, Nuclear Systems I: Thermal Hydraulic Fundamentals, Taylor & Francis, New York, NY, USA.
[51] A. Hébert, D. Sekki, and R. Chambon, 2012, "A User Guide for DONJON Version 4 (Technical Report IGE-300)", École Polytechnique de Montréal, Montreal, QC, Canada.
[52] S. Sahin, H. Yapıcı, and M. Bayrak, 1999, "Spent Mixed Oxide Fuel Rejuvenation in Fusion Breeders", Fusion Engineering and Design, 47, pp. 9–23. doi: 10.1016/S0920-3796(99)00066-6.
[53] X-5 Monte Carlo Team, 2003, "MCNP—A General Monte Carlo N-Particle Transport Code, Version 5", LA-UR-03-1987, Los Alamos National Laboratory, Los Alamos, NM, USA.
[54] A.V. Colton, B.P. Bromley, and S. Golesorkhi, 2017, "Assessment of Near-Breeding Heterogeneous Seed/Blanket Cores in Pressure-Tube Heavy Water Reactors with Thorium-Based Fuels", ANS Transactions, 116, pp. 97–102.
[55] S. Golesorkhi, B.P. Bromley, and M.H. Kaye, 2016, "Simulations of a Pressure-Tube Heavy Water Reactor Operating on Near-Breeding Thorium Cycles", Nuclear Technology, 194(2), pp. 178–191. doi: 10.13182/NT15-30.
[56] B.P. Bromley, A.V. Colton, and O. Collins, 2017, "Performance Improvements for Thorium-Based Fuels in Pressure Tube Heavy Water Reactors", CNL Nuclear Review, 6(2), pp. 161–173.